A new numerical approach for determining optimal thrust curves of masonry arches

A NEW NUMERICAL APPROACH FOR DETERMINING OPTIMAL THRUST CURVES OF MASONRY ARCHES

Eleonora Ricci[a], *Aguinaldo Fraddosio*[b,*], *Mario Daniele Piccioni*[b], *Elio Sacco*[c]

[a]*University of Cassino and Southern Lazio, viale dell'Università, 03043 Cassino, Italy*

[b]*Politechnic University of Bari, via Re David, 70125 Bari, Italy*

[c]*University of Naples Federico II, Via Claudio 21, 80125 Napoli, Italy*

[*]*Corresponding author. Politechnic University of Bari, via Re David, 70125 Bari, Italy Tel.: þ39 080 596 3738.*

E-mail addresses: e.ricci@unicas.it (E. Ricci), aguinaldo.fraddosio@poliba.it (A. Fraddosio), mariodaniele.piccioni@poliba.it (M.D. Piccioni), elio.sacco@unina.it (E. Sacco).

Abstract

In this paper a new numerical approach for determining admissible thrust curves for masonry arches is proposed. Arbitrary loading conditions, including distributed loads applied to the extrados and intrados of the arch, but also horizontal inertial forces simulating the effects of seismic actions are considered for arches characterized by any geometry. The admissible solutions, corresponding to equilibrium thrust curves entirely contained in the thickness of the arch, are consistent with the lower bound theorem of Limit Analysis and, thus, are "safe" solutions from a structural point of view. The well-established Milankovitch's theory for the equilibrium of masonry arches is reviewed and generalized. Then, a specific formulation of the theory is presented, allowing the construction of an effective and efficient numerical procedure based on the Point Collocation Method and enriched by a constrained optimization routine. The latter is aimed at determining, among all the admissible equilibrium solutions, the optimal solution matching specific requirements of interest for applications, as the solution corresponding to the maximum or minimum thrust. The proposed procedure is discussed and validated with reference to the cases of circular, parabolic and pointed arches. In particular, maximum and minimum thrust solutions have been determined for all the examined cases.

Keywords: Masonry arch; Thrust curve; Collocation Method.

1. Introduction

Masonry arches are very important and iconic structural elements of masonry constructions. Despite the large diffusion and the age-old history of masonry arches, the analysis of the structural response and the development of suitable theories for their design and for the determination of the structural

safety of masonry arches became a subject of study for researchers only in the XVII Century. From that moment on, the researches on the statics of masonry arches (and vaults) gave birth to a debate that intertwined and benefited from the development of the elastic theory in the XIX century, sometimes in a contradictory way (Benvenuto, 1981).

Among the cornerstones in the story of the research on the statics of masonry arches, it is worth to recall the seminal contribution by Robert Hooke who stated in 1675, in the form of an anagram, that "*As hangs the flexible line, so but inverted will stand the rigid arch*"[1]. In other words, he stated that if a cable fixed at both the extremities is left hanging under its self-weight, the cable takes the shape that, once inverted, an arch should have in order to withstand its self-weight (Hooke, 1676). This shape is called *catenary* and its mathematical expression was determined in the 1704 by Jacques Bernoulli, by imposing the equilibrium of infinitesimal part of the arch. Twenty years after Hooke's discovery, David Gregory (Gregory, 1698) stated that also the converse proposition is true: *"an arch of any form can only be in equilibrium if we can draw a catenary curve which passes through it"*. This concept is very important as it provides a way for evaluating the safety of a masonry arch (under the self-weight); moreover, Gregory gives indications for determining the horizontal thrust of the arch on its abutments.

These first attempts were based only on equilibrium, assuming only the action of the self-weight and that the material can sustain only compressive stresses. Moreover, the major result of the first studies was, generally, the determination of the thrust line, defined as the locus of points at which the resultant of the forces acting on the arch are applied. The thrust line is still today a key concept for the understanding of the mechanics of masonry arches. However, there is no a unique thrust line for a masonry arch under certain external loads, since the problem is statically indeterminate. Thus, suitable boundary conditions have to be prescribed.

Many authors, such as (de La Hire, 1695)(de La Hire, 1720)(Couplet, 1731)(Couplet, 1732) and (Méry, 1840) provided criteria for identifying the required boundary conditions, that is, for fixing points at which the thrust line must pass through or initial values of the horizontal component of the thrust. The approach could be static, see (Coulomb, 1776), or kinematic, as the one proposed by (Mascheroni, 1785), who determined the load bearing capacity of a masonry arch by applying the principle of virtual work in the condition of impending collapse of the arch. Up to that moment it was clear that an arch for which it was possible to draw different equilibrium thrust lines contained in its thickness was in any case “stable”, that is, capable of sustaining safely the applied loads (Block et al., 2006).

In XIX century the emerging Elasticity Theory drove researchers towards the problem of

[1] *Ut pendet continuum flexible sic stabit contigiuum rigidum inversum.*

determining the actual thrust line under assigned loads; this corresponds to the evaluation of the actual stress distribution in the arch, viewed as a statically indeterminate structure (Navier, 1826). Nevertheless, engineers were somehow reluctant to apply to masonry arches a theory that assumed the material to be isotropic, homogeneous and with well-defined elastic properties, since the knowledge of the building technique of masonry arches and vaults clearly show that those hypotheses actually do not apply. Anyway, until the beginning of the XX century, Elasticity Theory was considered the most suitable approach for studying the response of masonry arches, so that the need of determining the actual thrust line for assessing the equilibrium of an arch was considered an indisputable fact (Huerta, 2004).

In this context, the work of the Serbian engineer M. Milankovitch[2] is an exception, since Milankovitch turned again to the static approach, based only on the equilibrium, for the structural analysis of masonry arches. His work (Milanković, 1904) and (Milanković, 1907) provided for the first time a general and rigorous treatment of the problem of the equilibrium of masonry arches from a physical and mathematical point of view (Foce, 2007). But, in the history of structural analysis of masonry arches Milankovitch's contribution has been somehow kept in the shadow. Milankovitch himself, after publishing his doctoral thesis and two papers on this subject, left aside the problem of the equilibrium of masonry arches to deal with completely different issues. Nevertheless, Milankovitch's work is valuable for the mathematical treatment and worthy of attention. Notice that in Milankovitch's theory also external loads applied to the extrados and intrados are considered in addition to the self-weight. This makes the approach versatile, as the author himself demonstrated by analyzing special cases (e.g. the design of a retaining wall) and providing analytical solutions, when available. However, no method or indications are given to solve the equilibrium differential equations, somewhat complex, for more general cases.

After a period of lower interest, the subject of the mechanics of masonry structures has progressively gained more and more relevance during the last decades, since a new concern toward the preservation and the strengthening of historical construction arise, driven also by severe damages observed in masonry constructions after earthquakes (Roca et al., 2010). New studies have focalized the fact that in order to understand the actual mechanical response of masonry structures complex models considering plasticity, damage, fracture and contact, studied trough advanced numerical methods, are needed (Luciano and Sacco, 1998)(Addessi et al., 2010)(Milani and

[2] Milutin Milanković (1879-1958) was a figure characterized by a wide spectrum of scientific interests for his time: he was a mathematician, astronomer, climatologist, geophysicist, civil engineer and popularizer of science. Beside the work about the equilibrium of masonry arches, here discussed, and the contributions in the field of Civil Engineering, he gave major contributions in the nascent science of Climatology. Among them, he characterized the climates of all the planets of the Solar system, and studied Earth's long-term climate changes caused by changes in the position of the Earth in comparison to the Sun.

Lourenço, 2012)(Addessi and Sacco, 2014)(Tralli et al., 2014)(Drougkas et al., 2016)(Lucchesi et al., 2018). Beside Finite Element Method (FEM) implementations, also the Discrete Element Method (DEM) was extensively studied for investigating the mechanical behavior of masonry constructions, especially for what concerns the response to dynamical loads (Livesley, 1978)(Lemos, 2007)(Sarhosis et al., 2014)(Baraldi et al., 2015)(Baraldi and Cecchi, 2016). Moreover, specific approaches have been recently developed for the analysis of masonry arches and vaults reinforced by FRP and FRCM composite materials (Fabbrocino et al., 2015)(Pintucchi and Zani, 2016)(Bertolesi et al., 2018a, 2018b)(Alecci et al., 2017, 2016a, 2016b).

At the same time, starting from the pioneering work by J. Heyman (Heyman, 1966) a very interesting point of view on the structural analysis of masonry constructions opened the way to a broad application of the Limit Analysis theory (Lubliner, 1990) for determining the load bearing capacity of masonry constructions and specifically of masonry arches. In particular, according to Heyman approach it is possible to reread the classical equilibrium theories for masonry arches in the rational framework of the well-known *safe theorem* of Limit Analysis (O'Dwyer, 1999) (Gilbert, 2007) (Block and Ochsendorf, 2008).

In recent years several studies have widely extended the capability of Limit Analysis for masonry structures both by new theoretical developments (Angelillo et al., 2014; Fortunato et al., 2017, 2016) and by revisiting old theories in the light of the current theoretical knowledge. In particular, several research contributions have focalized on the determination of collapse loads for masonry arches (Pintucchi and Zani, 2009) (Oliveira et al., 2010) (D'Altri et al., 2018) and on the determination of the thrust line for masonry arches (Huerta, 2006) (Varma et al., 2010) (Sacco, 2015).

In this vein, also Milankovitch's approach has been recently rediscovered and reconsidered (Ageno et al., 2004) (Foce, 2007) (Nikolić, 2016), also as the theoretical base for new and efficient numerical methods aimed at determining optimal thrust lines for masonry arches (Ricci et al., 2016).

In this paper, the Milankovitch's theory for the equilibrium of masonry arches is generalized by considering also inertial forces simulating the maximum effects of seismic actions, in addition to the already general load conditions considered by Milankovitch. Moreover, a suitable formulation of equilibrium equations is proposed allowing for constructing a numerical method for determining optimal admissible thrust line solutions for arches characterized by any geometry.

In particular, in Section 2 Milankovitch's theory is generalized for what concerns the geometrical description and the loading conditions: indeed, the geometrical description is referred to the mid-line of the arch, and horizontal inertial forces proportional to the self-weight, representative of

seismic actions, are added. In Section 3, a new formulation of the equilibrium equations in Cartesian coordinates is provided; the use of the Cartesian coordinates reveals to be very convenient for applications at least for two reasons: the geometry of the arch is usually determined by a survey, and, then, known in terms of Cartesian coordinates, and the proposed numerical implementation of the equilibrium equations becomes clearer and simpler.

Anyway, the complexity of the obtained differential equilibrium problem renders analytical solutions infeasible, except for very simple and basic cases. Therefore, in Section 4 a numerical method has been formulated for the determination of particular thrust lines, of interest for applications. This method is based on a suitable implementation of the Point Collocation Method (PCM) (Iserles, 1996) and on a constrained optimization procedure; the latter is aimed at determining particular admissible solutions like the maximum and minimum thrust lines, the geometric safety factor, etc.. In Section 5, the effectiveness of the proposed procedure has been verified considering the case of a circular arch subjected to self-weight; the maximum and minimum thrust lines have been studied and a comparison between the numerical solution and the available analytical one has been performed. Then, the proposed method has been applied for determining the maximum and minimum thrust lines for a parabolic arch. For this case, not usually taken into consideration in the literature, no analytical solutions are available; in particular, the proposed procedure is validated by comparing the results with those obtained by a FEM routine based on the Timoshenko's beam theory for elastic no-tension materials. Finally, the determination of the maximum and minimum thrust lines for a pointed arch is studied; also in this case, the validation of the procedure has been performed by the comparison with the results obtained by the above FEM routine.

In all the examined cases the results determined by the proposed approach are practically coincident with those considered for the validation: this shows the effectiveness of the innovative approach here presented; moreover, the case of the parabolic arch shows the versatility of the method in solving also problems of arches characterized by variable curvature.

2. A generalization of Milankovitch's equilibrium theory

Here Milankovitch's theory for the equilibrium of masonry arches is revisited in order to provide a more general formulation of the problem; equilibrium equations are expressed in local polar coordinates as originally proposed by Milankovitch. The generalization involves the geometrical description and the loading conditions; moreover, it also aimed to frame the Milankovitch's equations in the theory of Limit Analysis applied to masonry structures. In fact, according to

(Heyman, 1966), Limit Analysis may be applied to masonry structures under the following assumptions: a) masonry has no tensile strength; b) masonry has infinite compressive strength; c) sliding between masonry units cannot occur. In particular, the Lower Bound theorem of Limit Analysis states that a masonry structure subjected to assigned external loads does not collapse (or, eventually, is in incipient collapse condition) if it is possible to find a statically admissible stress field, that is, a stress field in equilibrium with the applied loads and obeying the above assumptions. In particular, for the assumptions a) and b) a statically admissible stress field can be represented by a thrust line in equilibrium with the applied loads and entirely contained within the thickness of the arch (Como, 2016). Thus, the definition of such a statically admissible thrust line is independent of the actual position and direction of the joints in the masonry. In order to satisfy also assumption c), the check that the friction is sufficient to prevent the joint from sliding has to be performed. This check it is generally verified for thin arches subjected only to vertical loads with the joints having pseudo-radial directions, but could be not satisfied when the thrust line results very inclined with respect to the normal direction to an actual joint.

Let a masonry arch of generic shape and constant width[3] t be considered, as schematically represented in **Error! Reference source not found.**1. While in Milankovitch's work (Milankovitch, 1907) the attention is focused on a voussoir defined by joints inclined according to the stereotomy of the arch, herein an infinitesimal element of arch delimited by cross-sections, orthogonal to the mid-line, is considered. The typical cross-section is inclined with respect to the vertical direction (y direction) by an angle θ. By assigning the mid-line function $y_m(\theta)$ and the thickness of the cross-section $d(\theta)$, the arch geometry is completely defined. Since the arch shape is generic, the center of curvature C(x_C,y_C) and the radius of curvature R_m may vary as the cross-section varies; the distances of the extrados line and of the intrados line from C along the direction of the radius of curvature are $R_{ex} = R_m + \frac{1}{2}d$ and $R_{in} = R_m - \frac{1}{2}d$, respectively. Finally, the R denotes the distance of the thrust line from C for the considered cross-section.

The thrust line can be represented in the "local" polar reference system C(R,θ) or in a global polar reference system O$\left(\hat{R},\varphi\right)$, with φ representing the inclination of OE on the vertical axis y, where E is the point of the thrust line belonging to the considered cross-section and $\hat{R}$ is the distance of E from the origin O (see **Error! Reference source not found.**1).

[3] In what follows it is assumed that the width t of the arch orthogonally to its mid plane is constant, but it is easy to further generalize the formulation by removing this hypothesis.

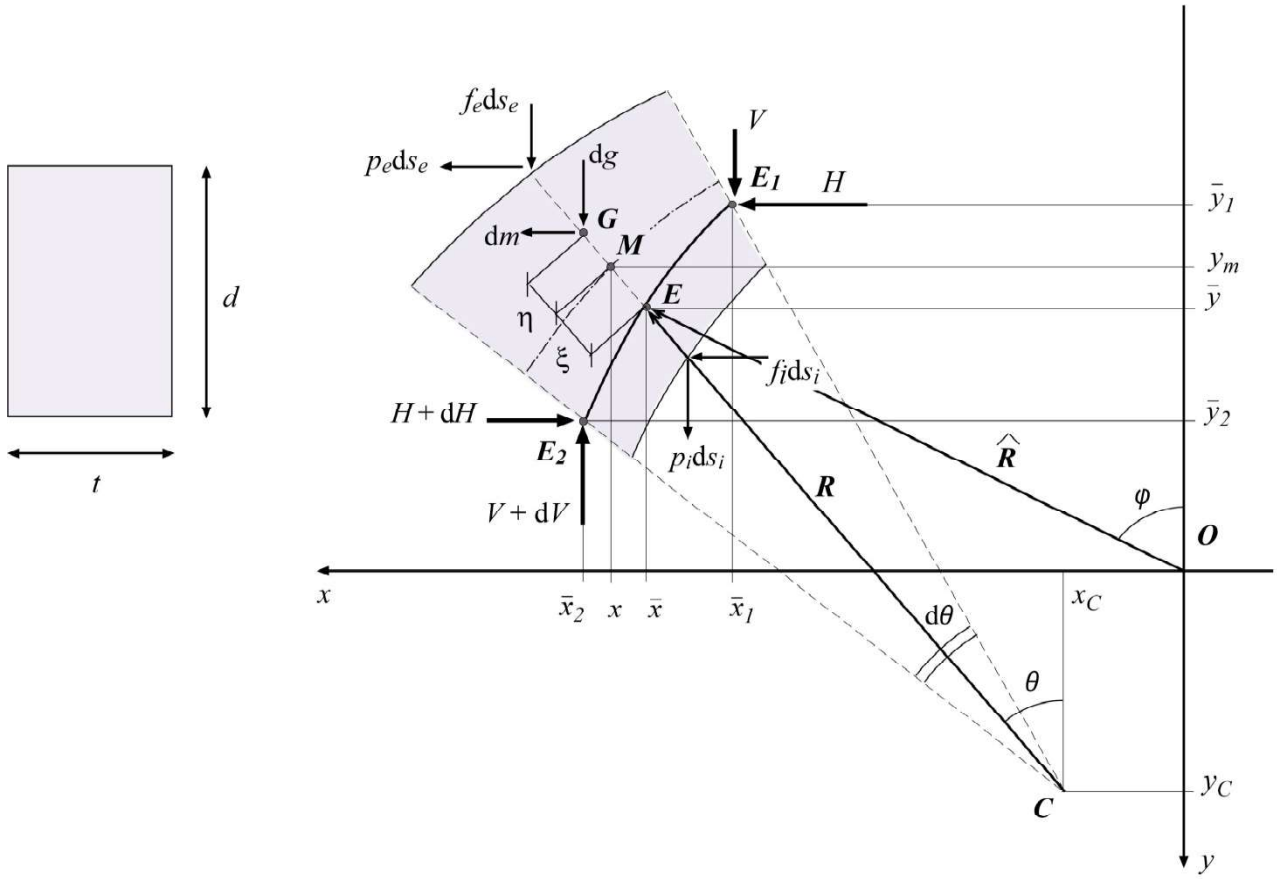

Fig. 1. Geometry and loading conditions of an infinitesimal voussoir of the arch.

Notice that from now on, when not necessary in terms of understanding, the dependence on θ is omitted in the expressions.

With reference to Fig. 2 an infinitesimal arch voussoir around the generic cross-section AB is a neighborhood of AB with amplitude dθ. A crucial observation for subsequent developments is that the center of mass G of the infinitesimal arch voussoir is different from the middle point M of the cross-section AB. In order to determine the position of G it is possible to consider the difference between the first moment of areaof the infinitesimal triangles CB_1B_2 and CA_1A_2 with respect to the axis passing through C and orthogonal to the radius of curvature. In particular, the first moment of area S_1 of CB_1B_2 is given by the area $A_{CB_1B_2}$ multiplied by the distance $R_{CB_1B_2}$ of its center of mass from C:

$$S_1 = A_{CB_1B_2}\, R_{CB_1B_2} = A_{CB_1B_2}\, \frac{2}{3}\left(R_m + \frac{d}{2}\right). \tag{1}$$

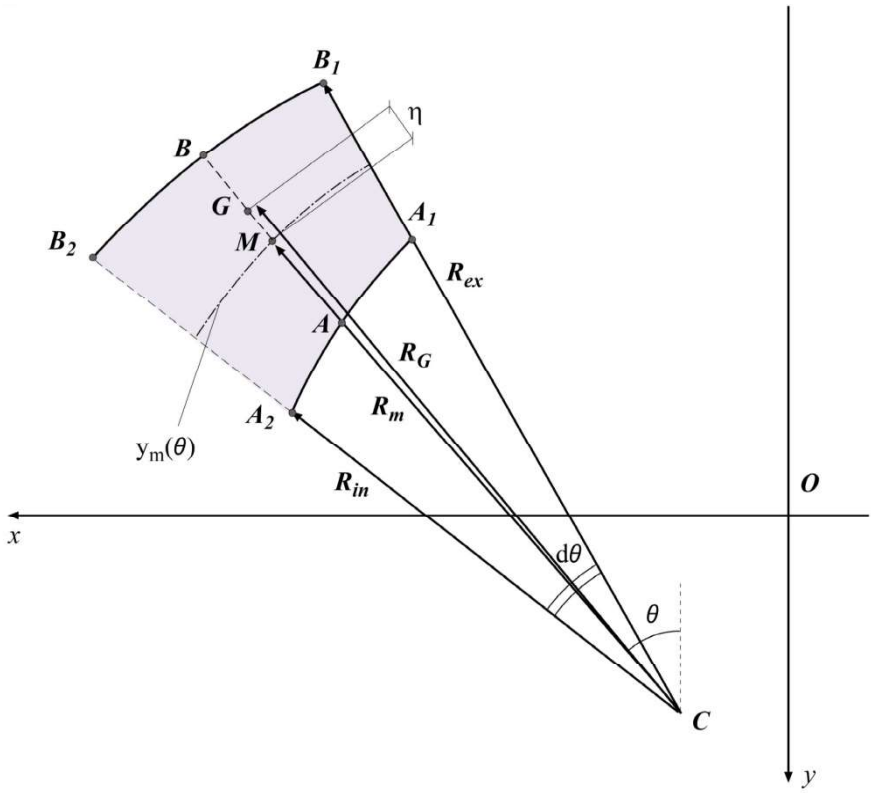

Fig. 2. Determination of the center of mass of an infinitesimal voussoir of the arch.

Similarly, the first moment of area S_2 of CA_1A_2 is given by the area $A_{CA_1A_2}$ multiplied by the distance $R_{CA_1A_2}$ of its center of mass from C:

$$S_2 = A_{CA_1A_2}\, R_{CA_1A_2} = A_{CA_1A_2}\, \frac{2}{3}\left(R_m - \frac{d}{2}\right). \tag{2}$$

Finally, the first moment of area of the infinitesimal voussoir $A_1B_1A_2B_2$ is:

$$\left(A_{CB_1B_2} - A_{CA_1A_2}\right) R_G = A_{CB_1B_2}\, \frac{2}{3}\left(R_m + \frac{d}{2}\right) - A_{CA_1A_2}\, \frac{2}{3}\left(R_m - \frac{d}{2}\right), \tag{3}$$

with R_G the distance of G from C. The ratio between the areas $A_{CB_1B_2}$ and $A_{CA_1A_2}$ is proportional to the ratio between the squares of the distances $\frac{2}{3}\left(R_m + \frac{d}{2}\right)$ and $\frac{2}{3}\left(R_m - \frac{d}{2}\right)$; therefore, it results:

$$A_{CB_1B_2} = A_{CA_1A_2}\, \frac{\left(R_m + \frac{d}{2}\right)^2}{\left(R_m - \frac{d}{2}\right)^2} \tag{4}$$

By substituting formula (4) in equation (3) and by solving with respect to R_G, it results:

$$R_G = R_m + \frac{d^2}{12R_m}. \tag{5}$$

Thus, the distance of the center of mass G of an infinitesimal voussoir with respect to its mid-line point M is obtained as:

$$\eta = \frac{d^2}{12R_m}. \tag{6}$$

For what concerns the loading conditions, the infinitesimal voussoir is assumed to be subjected to the self-weight, dg, applied to the center of mass G, and to arbitrary external loads acting at the extrados and the intrados of the arch. Similarly to Milankovitch, the latter loads are continuous regular functions of θ; in particular, the horizontal and vertical components of the external loads acting at the extrados of the arch are described by the functions $p_e(\theta)$ and $f_e(\theta)$, respectively, whereas the horizontal and vertical components of the external loads acting at the intrados of the arch are described by the functions $p_i(\theta)$ and $f_i(\theta)$, respectively. The self-weight can be expressed as:

$$\mathrm{d}g = \gamma\, t\, \frac{1}{2}\left(R_{ex}^2 - R_{in}^2\right)\mathrm{d}\theta, \tag{7}$$

with γ is the specific weight and $\frac{1}{2}\left(R_{ex}^2 - R_{in}^2\right)\mathrm{d}\theta$ the area of the infinitesimal voussoir.

In addition with respect to the Milankovitch's formulation the infinitesimal voussoir can be subjected also to horizontal inertial forces, dm, applied to the center of mass G. In particular, the inertial force dm is supposed to be proportional to the self-weight according to the following expression:

$$\mathrm{d}m = \gamma_h\, t\, \frac{1}{2}\left(R_{ex}^2 - R_{in}^2\right)\mathrm{d}\theta \tag{8}$$

where an apparent density γ_h proportional to γ is introduced. Notice that in the spirit of the conventional static analysis method for structures under seismic loads, the ratio γ_h/γ represents the maximum horizontal acceleration expected on the arch, according to the design seismic actions to be considered.

Let H and V be the horizontal and the vertical components of the resultant force acting on the right section of the considered infinitesimal voussoir, respectively, and let $H + \mathrm{d}H$ and $V + \mathrm{d}V$ be the horizontal and the vertical components of the resultant force applied on the left section of the infinitesimal voussoir, respectively. The translational equilibrium of the considered infinitesimal voussoir in the horizontal direction provides the following equation:

$$\left[(H+\mathrm{d}H)-H\right]-\mathrm{d}m-p_e\ \mathrm{d}s_e-p_i\ \mathrm{d}s_i=0. \tag{9}$$

Taking into account that the lengths of the extrados and intrados arches may be expressed as:

$$\mathrm{d}s_e=R_{ex}\ \mathrm{d}\theta,\qquad \mathrm{d}s_i=R_{in}\ \mathrm{d}\theta\,, \tag{10}$$

equation (9) takes the form:

$$\frac{\mathrm{d}H}{\mathrm{d}\theta}-\frac{1}{2}\ \gamma_h\ t\ \left(R_{ex}^2-R_{in}^2\right)-p_e\ R_{ex}+p_i\ R_{in}=0\,. \tag{11}$$

In a similar way, the translational equilibrium of the infinitesimal voussoir along the vertical direction *y* yields:

$$\left(V+\mathrm{d}V\right)-V-\mathrm{d}g-f_e\ \mathrm{d}s_e-f_i\ \mathrm{d}s_i=0; \tag{12}$$

that, accounting for equations (7) and (10), becomes:

$$\frac{\mathrm{d}V}{\mathrm{d}\theta}-\frac{1}{2}\ \gamma\ t\ \left(R_{ex}^2-R_{in}^2\right)-f_e\ R_{ex}-f_i\ R_{in}=0\,. \tag{13}$$

The rotational equilibrium of the infinitesimal voussoir about the point E, belonging to the thrust line (see Fig. 1), gives:

$$\begin{aligned}&V\ \mathrm{d}\overline{x}-H\ \mathrm{d}\overline{y}-\mathrm{d}g\ \left(\eta+\xi\right)\ \sin\theta-\mathrm{d}m\ \left(\eta+\xi\right)\ \cos\theta\\&-f_e\ \mathrm{d}s_e\ \left(\frac{d}{2}+\xi\right)\ \sin\theta-p_e\ \mathrm{d}s_e\ \left(\frac{d}{2}+\xi\right)\ \cos\theta\\&+f_i\ \mathrm{d}s_i\ \left(\frac{d}{2}-\xi\right)\ \sin\theta+p_i\ \mathrm{d}s_i\ \left(\frac{d}{2}-\xi\right)\ \cos\theta=0,\end{aligned} \tag{14}$$

with $\overline{x}\left(\theta\right)$ and $\overline{y}\left(\theta\right)$ the coordinates of the thrust line point E in the Cartesian reference system, and

$$\xi=R_m-R\,, \tag{15}$$

the eccentricity of the thrust line, i.e., the distance of the thrust line from the mid-line along the curvature radius, to be determined; with reference to Fig. 1, ξ is positive when the thrust line lies below the mid-curve. Because of equations (6), (8) and (10), the rotational equilibrium differential equation takes the form:

$$\begin{aligned}&V\frac{d\overline{x}}{d\theta}-H\frac{d\overline{y}}{d\theta}-\frac{1}{2}\ \gamma\ \mathrm{t}\ \left(R_{ex}^2-R_{in}^2\right)\ \left(\frac{d^2}{12R_m}+\xi\right)\ \sin\theta\\&-\frac{1}{2}\ \gamma_h\ \mathrm{t}\ \left(R_{ex}^2-R_{in}^2\right)\ \left(\frac{d^2}{12R_m}+\xi\right)\ \cos\theta-f_e\ R_{ex}\ \left(\frac{d}{2}+\xi\right)\ \sin\theta\\&-p_e\ R_{ex}\ \left(\frac{d}{2}+\xi\right)\ \cos\theta+f_i\ R_{in}\ \left(\frac{d}{2}-\xi\right)\ \sin\theta+p_i\ R_{in}\ \left(\frac{d}{2}-\xi\right)\ \cos\theta=0,\end{aligned} \tag{16}$$

The thrust line coordinates $\bar{x}$ and $\bar{y}$ may be expressed as functions of R and θ as:

$$\bar{x} = R\ \sin\theta + x_C, \qquad \bar{y} = -R\ \cos\theta + y_C, \tag{17}$$

and then their first derivative with respect to θ can be determined as:

$$\frac{\mathrm{d}\bar{x}}{\mathrm{d}\theta} = R\ \cos\theta + \frac{\mathrm{d}R}{\mathrm{d}\theta}\ \sin\theta, \qquad \frac{\mathrm{d}\bar{y}}{\mathrm{d}\theta} = R\ \sin\theta - \frac{\mathrm{d}R}{\mathrm{d}\theta}\ \cos\theta\,. \tag{18}$$

Taking into account formulae (17) and (18), equations (11), (12) and (14) form a system of three nonlinear differential equations in the variable θ whose unknowns are the thrust components $H(\theta)$, $V(\theta)$ and the radius $R(\theta)$; the latter determines the position of the thrust line. Solutions can be found by integrating these equations together with suitable boundary conditions.

The complexity of this differential problem makes it possible to find closed form solutions only in some special and simplified cases. Indeed, in his PhD thesis (Milankovitch, 1904) Milankovitch provided closed form solutions for some representative cases for specific geometries and loading conditions.

The equilibrium equations derived above are written in terms of the angle θ defined in the "local" polar reference system C(R, θ), whose center is the curvature center C. For switching from the local reference system to the global one O$\left(\hat{R}, \varphi\right)$, the following relations hold:

$$\begin{aligned} R_m\ \sin\theta &= \hat{R}_m\ \sin\varphi - x_C \\ R_m\ \cos\theta &= \hat{R}_m\ \cos\varphi + y_C. \end{aligned} \tag{19}$$

From (19) it is possible to determine θ and R_m as function of the angle φ and of $\hat{R}_m$:

$$\theta = \arctan\left(\frac{\hat{R}_m\ \sin\varphi - x_C}{\hat{R}_m\ \cos\varphi + y_C}\right) \qquad R_m = \frac{\hat{R}_m\ \cos\varphi + y_C}{\cos\theta}, \tag{20}$$

provided that $\hat{R}_m\ \cos\varphi + y_C \neq 0$ and $\cos\theta \neq 0$. Equations (20) are very useful when dealing with polycentric arches whose curvature centers are known a priori, as those represented in Fig. 3.

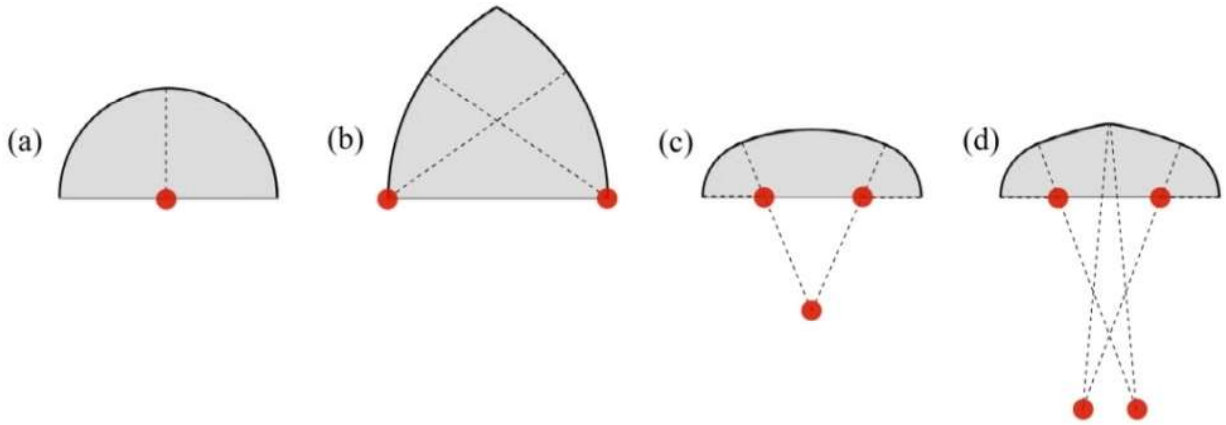

Fig. 3. One-centered arch (circular arch); (b) two-centered arch (pointed arch); (c) three-centered arch (basket-handle arch); four-centered arch (Tudor arch).

On the other hand, if a parabolic arch is considered, the curvature continuously varies from section to section; therefore, a formulation of the equilibrium equations in Cartesian coordinates may be more convenient for applications. The latter formulation is provided in the next Section.

3. Formulation of the equilibrium equations in a Cartesian reference system

In a Cartesian reference system $\mathrm{O}(x,y)$ the typical point of the mid-line of an arbitrary masonry arch is denoted by $\mathrm{M} \equiv (x_m, y_m)$ with $x_m(x) = x$; thus, the geometry of the arch is defined by assigning the mid-curve function, $y_m(x)$ and the thickness $d(x)$, see Fig. 1. The extrados and the intrados functions, $y_{ex}(x)$ and $y_{in}(x)$ can be determined by the function $d(x)$ by simple geometrical calculations.

The curvature $k_m(x)$ at the point M may be determined as:

$$k_m(x) = \frac{y_m''(x)}{\left(1 + \left(y_m'(x)\right)^2\right)^{3/2}}, \tag{21}$$

with

$$y_m'(x) = \frac{dy_m(x)}{dx}, \qquad y_m''(x) = \frac{d^2 y_m(x)}{dx^2} \tag{22}$$

where the prime indicates the derivative with respect to x.

Once the curvature is known, the mid-line radius (radius of curvature) $R_m(x)$ can be easily determined as the absolute value of the reciprocal of the curvature, i.e.:

$$R_m(x) = \frac{1}{|k_m(x)|} = \frac{\left(1 + \left(y'_m(x)\right)^2\right)^{3/2}}{|y''_m(x)|}. \tag{23}$$

The center of curvature $C\left(x_C(x), y_C(x)\right)$ of the considered cross-section is the point having the following coordinates:

$$\begin{aligned} x_C(x) &= x - R_m(x)\ \sin\theta(x) \\ y_C(x) &= y_m(x) + R_m(x)\ \cos\theta(x), \end{aligned} \tag{24}$$

where:

$$\theta(x) = \arctan\left(y'_m(x)\right). \tag{25}$$

With reference to Fig. 1, the position of the center of mass G is given by its distance $R_G(x)$ from M along the radius of curvature $R_m(x)$ according to equation (5). For the next developments it is also useful to observe that:

$$\frac{\mathrm{d}\theta}{\mathrm{d}x} = \frac{y''_m}{1 + \left(y'_m\right)^2}, \tag{26}$$

and that:

$$\sin\theta(x) = \frac{y'_m(x)}{\sqrt{1 + \left(y'_m(x)\right)^2}}, \qquad \cos\theta(x) = \frac{1}{\sqrt{1 + \left(y'_m(x)\right)^2}}. \tag{27}$$

A crucial matter concerns the determination of the eccentricity $\xi(x)$ of the thrust line from the mid-line, measured along the radius of curvature, as a function of the independent variable *x*. Indeed, as shown in Fig. 1, once the angle θ is assigned the point E of the thrust line is determined by its distance $\xi(x)$ from the point M belonging to the mid-line. It results:

$$\xi(x) = \frac{x - \bar{x}(x)}{\sin\theta(x)} = -\frac{y_m(x) - \bar{y}(x)}{\cos\theta(x)}. \tag{28}$$

Hence, the parametric equation of the thrust line is given by assigning, for each *x*, the pair of coordinates $\left(\bar{x}(x), \bar{y}(x)\right)$ of the point E of the thrust line belonging to the cross-section centered in $M\left(x, y_m\right)$:

$$\begin{cases} \bar{x}(x) = x - \xi(x)\dfrac{y_m'(x)}{\omega(x)} \\ \bar{y}(x) = y_m(x) + \xi(x)\dfrac{1}{\omega(x)}, \end{cases} \tag{29}$$

with

$$\omega(x) = \sqrt{1 + \left(y_m'(x)\right)^2}\,. \tag{30}$$

From now on, the dependence on *x*, when non-essential in terms of understanding, it is omitted for lightening the expressions.

Let the considered infinitesimal voussoir be subjected to self-weight, d*g*, to inertial forces, d*m*, to horizontal and vertical loads applied to the extrados, $p_e \mathrm{d}s_e$ and $f_e \mathrm{d}s_e$, and intrados, $p_i \mathrm{d}s_i$ and $f_i \mathrm{d}s_i$, respectively. Since

$$\frac{1}{2}\left(R_{ex}^2 - R_{in}^2\right) = \mathrm{d}R_m, \tag{31}$$

from (8), (9) and (10) the translational equilibrium of the considered infinitesimal voussoir along *x* gives:

$$\frac{\mathrm{d}H}{\mathrm{d}x} - \gamma_h\, t\, d\, R_m \frac{\mathrm{d}\theta}{\mathrm{d}x} - p_e\, R_{ex} \frac{\mathrm{d}\theta}{\mathrm{d}x} - p_i\, R_{in} \frac{\mathrm{d}\theta}{\mathrm{d}x} = 0\,. \tag{32}$$

By (23), (26) and (30) equation (32) becomes:

$$\frac{\mathrm{d}H}{\mathrm{d}x} = \gamma_h\, t\, d\, \omega + \left(p_e + p_i\right)\omega + \frac{d}{2}\left(p_e - p_i\right)\frac{y_m''}{\omega}\,. \tag{33}$$

Similarly, by (9), (10) and (13) the translational equilibrium of the infinitesimal voussoir along *y* provides the following equation:

$$\frac{\mathrm{d}V}{\mathrm{d}x} - \gamma\, t\, d\, R_m \frac{\mathrm{d}\theta}{\mathrm{d}x} - f_e\, R_{ex} \frac{\mathrm{d}\theta}{\mathrm{d}x} - f_i\, R_{in} \frac{\mathrm{d}\theta}{\mathrm{d}x} = 0\,, \tag{34}$$

that may be written as:

$$\frac{\mathrm{d}V}{\mathrm{d}x} = \gamma\, t\, d\, \omega + \left(f_e + f_i\right)\omega + \frac{d}{2}\left(f_e - f_i\right)\frac{y_m''}{\omega}\,. \tag{35}$$

From the rotational equilibrium of the infinitesimal voussoir about E, it results:

$$\begin{aligned} &H\left(\bar{y}_2 - \bar{y}_1\right) + \mathrm{d}H\left(\bar{y}_2 - \bar{y}\right) - V\left(\bar{x}_2 - \bar{x}_1\right) - \mathrm{d}V\left(\bar{x}_2 - \bar{x}\right) + \mathrm{d}m\left(\xi + \frac{d^2}{12R_m}\right)\cos\theta + \mathrm{d}g\left(\xi + \frac{d^2}{12R_m}\right)\sin\theta + \\ &+ p_e\, \mathrm{d}s_e\left(\xi + \frac{d}{2}\right)\cos\theta + f_e\, \mathrm{d}s_e\left(\xi + \frac{d}{2}\right)\sin\theta - p_i\, \mathrm{d}s_i\left(\frac{d}{2} - \xi\right)\cos\theta - f_i\, \mathrm{d}s_i\left(\frac{d}{2} - \xi\right)\sin\theta = 0\,, \end{aligned} \tag{36}$$

where $\left(\overline{x}_1(x), \overline{y}_1(x)\right)$ and $\left(\overline{x}_2(x), \overline{y}_2(x)\right)$ are the coordinates of the intersections of the left cross-section and the right cross-section of the considered infinitesimal voussoir with the thrust line. It can be observed that:

$$\begin{aligned}
\overline{x}_1 &= x_C + \left[R_m - \left(\xi - \frac{\mathrm{d}\xi}{2}\right)\right]\sin\left(\theta - \frac{\mathrm{d}\theta}{2}\right), \\
\overline{x}_2 &= x_C + \left[R_m - \left(\xi + \frac{\mathrm{d}\xi}{2}\right)\right]\sin\left(\theta + \frac{\mathrm{d}\theta}{2}\right), \\
\overline{y}_1 &= y_C - \left[R_m - \left(\xi - \frac{\mathrm{d}\xi}{2}\right)\right]\cos\left(\theta - \frac{\mathrm{d}\theta}{2}\right), \\
\overline{y}_2 &= y_C - \left[R_m - \left(\xi + \frac{\mathrm{d}\xi}{2}\right)\right]\cos\left(\theta + \frac{\mathrm{d}\theta}{2}\right)
\end{aligned} \tag{37}$$

and that

$$\begin{aligned}
\sin\left(\theta - \frac{\mathrm{d}\theta}{2}\right) &= \sin\theta\ \cos\frac{\mathrm{d}\theta}{2} - \cos\theta\ \sin\frac{\mathrm{d}\theta}{2} \simeq \sin\theta - \frac{\mathrm{d}\theta}{2}\cos\theta, \\
\sin\left(\theta + \frac{\mathrm{d}\theta}{2}\right) &= \sin\theta\ \cos\frac{\mathrm{d}\theta}{2} + \cos\theta\ \sin\frac{\mathrm{d}\theta}{2} \simeq \sin\theta + \frac{\mathrm{d}\theta}{2}\cos\theta, \\
\cos\left(\theta - \frac{\mathrm{d}\theta}{2}\right) &= \cos\theta\ \cos\frac{\mathrm{d}\theta}{2} + \sin\theta\ \sin\frac{\mathrm{d}\theta}{2} \simeq \cos\theta + \frac{\mathrm{d}\theta}{2}\sin\theta, \\
\cos\left(\theta + \frac{\mathrm{d}\theta}{2}\right) &= \cos\theta\ \cos\frac{\mathrm{d}\theta}{2} - \sin\theta\ \sin\frac{\mathrm{d}\theta}{2} \simeq \cos\theta - \frac{\mathrm{d}\theta}{2}\sin\theta.
\end{aligned} \tag{38}$$

Therefore, after some calculations, it follows:

$$\begin{aligned}
\overline{x}_2 - \overline{x}_1 &= \left(R_m - \xi\right)\mathrm{d}\theta\ \cos\theta - \mathrm{d}\xi\ \sin\theta, \\
\overline{y}_2 - \overline{y}_1 &= \left(R_m - \xi\right)\mathrm{d}\theta\ \sin\theta + \mathrm{d}\xi\ \cos\theta
\end{aligned} \tag{39}$$

while

$$\overline{x}_2 - \overline{x} = x_C + \left[R_m - \left(\xi + \frac{\mathrm{d}\xi}{2}\right)\right]\left(\sin\theta + \frac{\mathrm{d}\theta}{2}\cos\theta\right) - \overline{x}\,. \tag{40}$$

From Fig. 1, it can be observed that:

$$\overline{x} = x_C + \left(R_m - \xi\right)\sin\theta \tag{41}$$

since the quantity $\mathrm{d}\xi\ \mathrm{d}\theta$ is negligible. Thus, equation (49) becomes:

$$\overline{x}_2 - \overline{x} = \left(R_m - \xi\right)\frac{\mathrm{d}\theta}{2}\cos\theta - \frac{\mathrm{d}\xi}{2}\sin\theta\,. \tag{42}$$

In a similar way, the quantity $\overline{y}_2 - \overline{y}$ can be determined, resulting:

$$\overline{y}_2-\overline{y}=y_C-\left[R_m-\left(\xi+\frac{\mathrm{d}\xi}{2}\right)\right]\left(\cos\theta-\frac{\mathrm{d}\theta}{2}\sin\theta\right)-\overline{y}= \\ =\left(R_m-\xi\right)\frac{\mathrm{d}\theta}{2}\sin\theta+\frac{\mathrm{d}\xi}{2}\cos\theta. \tag{43}$$

Thus, equation (36) can be written as follows:

$$H\left[\left(R_m-\xi\right)\mathrm{d}\theta\ \sin\theta-\mathrm{d}\xi\ \cos\theta\right]+\mathrm{d}H\left[\left(R_m-\xi\right)\frac{\mathrm{d}\theta}{2}\sin\theta+\frac{\mathrm{d}\xi}{2}\cos\theta\right]+ \\ -V\left[\left(R_m-\xi\right)\mathrm{d}\theta\ \cos\theta-\mathrm{d}\xi\ \sin\theta\right]-\mathrm{d}V\left[\left(R_m-\xi\right)\frac{\mathrm{d}\theta}{2}\cos\theta-\frac{\mathrm{d}\xi}{2}\sin\theta\right]+ \\ +\mathrm{d}g\left(\xi+\frac{d^2}{12R_m}\right)\sin\theta+\mathrm{d}p\left(\xi+\frac{d^2}{12R_m}\right)\cos\theta+p_e\ \mathrm{d}s_e\left(\xi+\frac{d}{2}\right)\cos\theta+ \\ +f_e\ \mathrm{d}s_e\left(\xi+\frac{d}{2}\right)\sin\theta-p_i\ \mathrm{d}s_i\left(\frac{d}{2}-\xi\right)\cos\theta-f_i\ \mathrm{d}s_i\left(\frac{d}{2}-\xi\right)\sin\theta=0. \tag{44}$$

The terms $\mathrm{d}V\left[\left(R_m-\xi\right)\frac{\mathrm{d}\theta}{2}\cos\theta-\frac{\mathrm{d}\xi}{2}\sin\theta\right]$ and $\mathrm{d}H\left[\left(\xi-R_m\right)\frac{\mathrm{d}\theta}{2}\sin\theta+\frac{\mathrm{d}\xi}{2}\cos\theta\right]$ in equation (44) can be neglected since infinitesimal of higher order with respect to the other terms. By taking into account formula (31), the following differential equilibrium equation is obtained:

$$\left(H\ \cos\theta+V\ \sin\theta\right)\frac{\mathrm{d}\xi}{\mathrm{d}x} \\ +\left\{\left[-H+\gamma\ R_m\ t\ d+\left(f_e\ R_{ex}+f_i\ R_{in}\right)\right]\sin\theta+\right. \\ \left.\left[V+\gamma_h\ R_m\ t\ d+\left(p_e\ R_{ex}+p_i\ R_{in}\right)\right]\cos\theta\right\}\frac{\mathrm{d}\theta}{\mathrm{d}x}\xi \\ +\left\{\left[H\ R_m+\gamma\ R_m\ t\ d\ \eta+\frac{d}{2}\left(f_e\ R_{ex}-f_i\ R_{in}\right)\right]\sin\theta+\right. \\ \left.\left[-V\ R_m+\gamma_h\ R_m\ t\ d\ \eta+\frac{d}{2}\left(p_e\ R_{ex}-p_i\ R_{in}\right)\right]\cos\theta\right\}\frac{\mathrm{d}\theta}{\mathrm{d}x}=0. \tag{45}$$

Substituting formulae (23), (26), (27) and (30) into (45), it results:

$$\left(H\frac{1}{\omega}+V\frac{y_m^{''}}{\omega}\right)\frac{\mathrm{d}\xi}{\mathrm{d}x}+\left[-H\frac{y_m^{'}\ y_m^{''}}{\omega^3}+V\frac{y_m^{''}}{\omega^3}+\gamma_h\ t\ d+\gamma\ t\ d\ y_m^{'}+\right. \\ \left.\left(f_e\ y_m^{'}+p_e\right)\left(1+\frac{y_m^{''}\ d}{2\omega^3}\right)+\left(f_i\ y_m^{'}+p_i\right)\left(1-\frac{y_m^{''}\ d}{2\omega^3}\right)\right]\xi+H\ y_m^{'}-V+ \\ \left(\gamma_h+\gamma\ y_m^{'}\right)\frac{t\ d^3}{12}\frac{y_m^{''}}{\omega^3}+\left(f_e\ y_m^{'}+p_e\right)\frac{d}{2}\left(1+\frac{y_m^{''}\ d}{2\omega^3}\right)-\left(f_i\ y_m^{'}+p_i\right)\frac{d}{2}\left(1-\frac{y_m^{''}\ d}{2\omega^3}\right)=0. \tag{46}$$

In conclusion, the equilibrium of the arch is described by the following system of three non-linear first order Ordinary Differential Equations (ODE):

$$\frac{\mathrm{d}H}{\mathrm{d}x}=\gamma_h\ t\ d\ \omega+\left(p_e+p_i\right)\omega+\frac{d}{2}\left(p_e-p_i\right)\frac{y_m^{''}}{\omega}$$

$$\frac{\mathrm{d}V}{\mathrm{d}x}=\gamma\ t\ d\ \omega+\left(f_e+f_i\right)\omega+\frac{d}{2}\left(f_e-f_i\right)\frac{y_m^{''}}{\omega}$$

$$\left(H\frac{1}{\omega}+V\frac{y_m^{''}}{\omega}\right)\frac{\mathrm{d}\xi}{\mathrm{d}x}+\left[-H\frac{y_m^{'}y_m^{''}}{\omega^3}+V\frac{y_m^{''}}{\omega^3}+\gamma_h\ t\ d+\gamma\ t\ d\ y_m^{'}+\right. \tag{47}$$

$$\left.\left(f_e\ y_m^{'}+p_e\right)\left(1+\frac{y_m^{''}\ d}{2\omega^3}\right)+\left(f_i\ y_m^{'}+p_i\right)\left(1-\frac{y_m^{''}\ d}{2\omega^3}\right)\right]\xi+H\ y_m^{'}-V+$$

$$\left(\gamma_h+\gamma\ y_m^{'}\right)\frac{t\ d^3}{12}\frac{y_m^{''}}{\omega^3}+\left(f_e\ y_m^{'}+p_e\right)\frac{d}{2}\left(1+\frac{y_m^{''}\ d}{2\omega^3}\right)-\left(f_i\ y_m^{'}+p_i\right)\frac{d}{2}\left(1-\frac{y_m^{''}\ d}{2\omega^3}\right)=0,$$

where the unknowns are the eccentricity of the thrust line, $\xi(x)$, the horizontal and vertical components of the resultant force, $H(x)$ and $V(x)$, respectively. All the other terms in (47) are known functions (or derivative of known functions).

Analytical solutions of ODE system (47) are prohibitive to be determined; thus, the development of suitable numerical methods is needed.

4. Numerical procedure for the determination of the thrust line

Herein, a suitable implementation of the Point Collocation Method (PCM) (Iserles, 1996) is adopted for the determination of numerical solutions of the ODE system (47).

The Point Collocation Method is a numerical approach particularly effective for solving ODE boundary value problems (BVP). Basically, it consists in approximating each unknown function with a polynomial of a certain degree, and in requiring that the polynomial approximation exactly satisfies the differential equations at a finite number n_p of discrete points, called collocation points, chosen within the domain of definition of the problem. It is readily seen that PCM is conceptually simple, which makes this method handy and versatile. The literature (e.g. Asher et at., 1995) provides also the optimal position of the collocation points in the domain, according to the degree of the approximating polynomial.

In the proposed implementation, the domain of definition of the problem is discretized in subdomains, and in each of them PCM is applied; thus, in addition to boundary conditions, continuity conditions between subdomains have to be imposed. By variating the number of the subdomains and the degree of the approximating polynomials it is possible to find an optimal balance between the accuracy of the numerical results and the computational effort.

In particular, the numerical procedure consists in the steps reported below.

1- The domain of definition of the ODE system (47) is discretized in n_e intervals $\Omega_i = \left[x_1^{(i)}, x_2^{(i)} \right]$, $i = 1,...,n_e$, through the introduction of $n_d = n_e + 1$ points; in Fig. 4 the typical interval of the discretization is depicted.

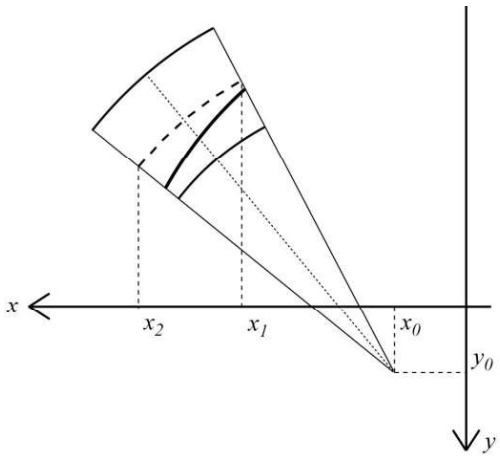

Fig. 4. The i-th interval subdividing the domain for the application of the point collocation method.

2- Within each interval Ω_i the unknown functions $H(x)$, $V(x)$ and $\xi(x)$ are approximated by polynomials, $H^{(i)}(x)$, $V^{(i)}(x)$ and $\xi^{(i)}(x)$; different degrees of the polynomial can be considered for each of the three unknown functions. In particular, it appears to be convenient to choose a polynomial of higher degree for approximating the eccentricity of the thrust line with respect to the mid-line, $\xi(x)$, and of lower degree for approximating the horizontal and vertical components of the thrust, $H(x)$ and $V(x)$. In particular, for the following case-studies polynomials of degree 2 are adopted for approximating $H(x)$ and $V(x)$:

$$\begin{aligned} H^{(i)}(x) &= h_1^{(i)} + h_2^{(i)}\, x + h_3^{(i)}\, x^2 \\ V^{(i)}(x) &= v_1^{(i)} + v_2^{(i)}\, x + v_3^{(i)}\, x^2 \end{aligned} \qquad i = 1,...,n_e \tag{48}$$

with $h_j^{(i)}$ and $v_j^{(i)}$, $j = 1,...,3$, coefficients of the polynomials. On the other hand, the function $\xi(x)$ is approximated by a polynomials of degree 4:

$$\xi^{(i)}(x) = r_1^{(i)} + r_2^{(i)} x + r_3^{(i)} x^2 + r_4^{(i)} x^3 + r_5^{(i)} x^4 \qquad i = 1,...,n_e \tag{49}$$

with $r_j^{(i)}$, $j = 1,...,5$ coefficients of the polynomial.

In such a way, a total number of unknown coefficients equal to $(3+3+5) \times n_e$ is introduced.

3- A suitable number of collocation points are defined within each interval Ω_i. In particular, for equations $(47)_1$ and $(47)_2$, involving only the unknown functions $H(x)$ and $V(x)$ that are approximated by polynomials of degree 2, the following two collocation points are considered:

$$x_{cp1}^{(i)} = x_1^{(i)} + \left(x_2^{(i)} - x_1^{(i)}\right)\left(\frac{1}{2} - \frac{\sqrt{3}}{6}\right) \qquad x_{cp2}^{(i)} = x_1^{(i)} + \left(x_2^{(i)} - x_1^{(i)}\right)\left(\frac{1}{2} + \frac{\sqrt{3}}{6}\right). \tag{50}$$

For what concerns equation $(47)_3$, involving also the unknown function $\xi(x)$ that is approximated by polynomials of degree 4, the following four collocation points are adopted:

$$\begin{aligned}
x_{cp1}^{(i)} &= x_1^{(i)} + \left(x_2^{(i)} - x_1^{(i)}\right)\left(\frac{1}{2} - \sqrt{\frac{3}{28} + \frac{1}{14}\sqrt{\frac{6}{5}}}\right) \\
x_{cp2}^{(i)} &= x_1^{(i)} + \left(x_2^{(i)} - x_1^{(i)}\right)\left(\frac{1}{2} - \sqrt{\frac{3}{28} - \frac{1}{14}\sqrt{\frac{6}{5}}}\right) \\
x_{cp3}^{(i)} &= x_1^{(i)} + \left(x_2^{(i)} - x_1^{(i)}\right)\left(\frac{1}{2} + \sqrt{\frac{3}{28} - \frac{1}{14}\sqrt{\frac{6}{5}}}\right) \\
x_{cp4}^{(i)} &= x_1^{(i)} + \left(x_2^{(i)} - x_1^{(i)}\right)\left(\frac{1}{2} + \sqrt{\frac{3}{28} + \frac{1}{14}\sqrt{\frac{6}{5}}}\right).
\end{aligned} \tag{51}$$

4- For the *i*-th interval Ω_i, the ODE system (47) have to be exactly satisfied at the *j*-th collocation point, which means that the residual has to be zero at that point. Notice that equations $(47)_1$ and $(47)_2$ are uncoupled and involve only the unknown functions $H(x)$ and $V(x)$, respectively. In particular, once for each interval the two collocation conditions are imposed at the points specified in (50), $2\times 2\times n_e$ algebraic equations are obtained. Moreover, by requiring that the differential equation $(47)_3$ is exactly satisfied by the polynomials at the 4 collocation points defined by formulae (51), further $4\times n_e$ algebraic equations are obtained. In conclusion, the collocation conditions lead to write $8\times n_e$ algebraic equations.

5- Continuity conditions are set at the nodes representing the connection between intervals:

$$\begin{aligned}
H^{(i-1)}(x_i) &= H^{(i)}(x_i) \\
V^{(i-1)}(x_i) &= V^{(i)}(x_i) \\
\xi^{(i-1)}(x_i) &= \xi^{(i)}(x_i)
\end{aligned} \tag{52}$$

with i=1,...,n_e-1. In such a way, further $3\times(n_e - 1)$ are written.

6- By the above steps, a system of $11\times n_e - 3$ equations in $11\times n_e$ unknowns is obtained. As consequence, the equilibrium problem results to be three times undetermined. A solution can be then determined in two different ways:
   - by imposing three boundary conditions on the three unknown functions,
   - by using suitable constrained optimization procedures aimed at determining specific solutions, among the possible ∞^3, having special relevance for applications.

For what concerns the latter approach, a possible constrained optimization problem may aims at determining the solution corresponding to the minimum or maximum value of the thrust force. To this end, it is required to minimize or maximize $H_0 = H^{(1)}(x_1)$, that is the thrust at the left impost, and to impose, for the sake of the admissibility, that the thrust line lies inside the thickness of the arch:

$$\min H_0 \;/\; \max H_0 \qquad \text{with} \begin{cases} \xi(x) \le +\dfrac{d}{2} \\ \xi(x) \ge -\dfrac{d}{2}. \end{cases} \tag{53}$$

Also the problem of the determination of the Geometric Safety Factor (GSF), i.e. the ratio between the actual thickness of the arch and the minimum thickness of a homothetic arch enveloping an equilibrium thrust line (O'Dwyer, 1999), can be faced. Analogously, by the optimization approach the study of arches with limited compressive strength or, vice-versa, with non-zero tensile strength due to reinforcements (e.g., FRP or FRCM reinforcements) can be addressed. In particular, from a geometrical point of view a limited compressive strength implies a narrowing of the domain in which a statically admissible thrust line should be contained (Nobile and Bartolomeo, 2014), whereas a non-zero tensile strength due to reinforcements implies that the above domain has to be conveniently extended (Alecci et al., 2016a). Finally, a constrained optimization routine may be employed for determining the maximum value of variable loads such that a statically admissible thrust line can be found, and then the value of the collapse load multiplier. Among possible variable loads, it is of paramount interest for applications the case of horizontal inertia loads: in this case, the seismic acceleration capable of determining the collapse of the arch may be determined (Block et al., 2006).

The procedure above described has been conveniently implemented by a code in Matlab© environment; the code allows for assigning all the functions required for determining the coefficients of the polynomials approximating the solutions of the ODE system (47); moreover, it is possible to choose the number of intervals in which the domain has to be subdivided and the degree of the polynomials approximating the unknown functions. Then, the code allows for choosing

between the assignment of explicit boundary conditions or the use of one of the optimization procedures above described. In the first case, the code assesses whether the thrust line actually lies inside the thickness of the arch. At the end, the code gives in correspondence of the found solution the values of the horizontal thrust and of the vertical action at the imposts, and it plots the related thrust line.

5. Numerical applications

In this Section numerical applications are developed to assess the effectiveness of the proposed procedure. In particular, these applications concern:

- the case of a circular arch, for which the solution determined by applying the proposed approach is compared with the analytical solution;
- the case of a parabolic arch, for which the solution determined by applying the proposed approach is compared with the solution determined by using a specific no-tension Finite Element Method (FEM) procedure;
- the case of a pointed arch, for which again the solution determined by applying the proposed approach is compared with the solution obtained by the above cited FEM procedure.

In all the above listed numerical applications, the problem of the minimum and maximum value of the thrust force is addressed.

5.1. Circular arch

Here, the classical case of a circular masonry arch is studied by applying the innovative approach proposed in this paper.

A circular arch characterized by the geometrical data reported in Table 1, is considered. The arch is subjected to only to the self-weight, so that the following positions are made:

$$\gamma(\theta) = \text{cost} = \gamma, \qquad \gamma_h(\theta) = f_e(\theta) = p_e(\theta) = f_i(\theta) = p_i(\theta) = 0 \tag{54}$$

In the examined case of a circular arch under the self-weight also analytical solutions can be determined, so that a comparison between the analytical solution and the numerical solution obtained by the proposed approach can be accomplished.

Table 1. Geometrical data of the circular arch.

C	R_m	d	t	R_{ex}	R_{in}	γ

[mm]	[mm]	[mm]	[mm]	[mm]	[mm]	[daN/mm^3]
(0,0)	1200	300	500	1350	1050	2000

For the specific geometry and loading condition, the system of equilibrium equations (47) becomes:

$$\begin{aligned} &\frac{dH}{dx}=0 \\ &\frac{dV}{dx}=\gamma\ t\ d\ R_m\frac{d\theta}{dx} \\ &\frac{1}{\omega}\left(H+V\ y_m^{''}\right)\frac{d\xi}{dx}+\left[-H\frac{y_m^{'}\ y_m^{''}}{\omega^3}+V\frac{y_m^{''}}{\omega^3}+\gamma\ t\ d\ y_m^{'}\right]\xi+H\ y_m^{'}-V+\gamma\ y_m^{'}\frac{t\ d^3}{12}\frac{y_m^{''}}{\omega^3}=0. \end{aligned} \tag{55}$$

From $(55)_1$ it follows that the horizontal component of the thrust is constant:

$$H=H_0\,. \tag{56}$$

Moreover, by integrating equation $(55)_2$, it results:

$$V=\gamma\ t\ d\ R_m\ \theta+k \tag{57}$$

with k an integration constant. Because of the symmetry of the problem, the vertical force V is zero on the symmetry axis, that is:

$$V\left(x=0\right)=V\left(\theta=0\right)=0\,. \tag{58}$$

This imply that in (57) $k=0$. Furthermore, by recalling formula (25), it results:

$$V=\gamma\ t\ d\ R_m\ \arctan\left(y_m^{'}\right). \tag{59}$$

Substituting expressions (58) and (59) in equation $(55)_3$, the following differential equation in $\xi\left(x\right)$ is obtained:

$$\frac{1}{\omega}\left(H_0+V\ y_m^{''}\right)\frac{d\xi}{dx}+\left[-H_0\frac{y_m^{'}\ y_m^{''}}{\omega^3}+V\frac{y_m^{''}}{\omega^3}+\gamma\ t\ d\ y_m^{'}\right]\xi+H_0\ y_m^{'}-V+\gamma\ y_m^{'}\frac{t\ d^3}{12}\frac{y_m^{''}}{\omega^3}=0\,, \tag{60}$$

with

$$y_m=100+\sqrt{1200^2-x^2}\qquad y_m^{'}=\frac{-x}{\sqrt{1200^2-x^2}}\qquad y_m^{''}=\frac{-x^2}{\sqrt{\left(1200^2-x^2\right)^3}}-\frac{1}{\sqrt{1200^2-x^2}}\,. \tag{61}$$

Since the solutions of $(55)_1$ and $(55)_2$ have been already determined analytically, the numerical method described in Section 5 is applied only for solving equation $(55)_3$. To this aim, the domain $x\in\left[-1200,1200\right]$ is divided into $n_e=16$ intervals of the same length, and for each of them the eccentricity $\xi\left(x\right)$ is approximated by a polynomial of the fourth degree. In each interval, four collocation conditions are imposed; these conditions, together with the continuity conditions $(52)_3$ yields a system of $5\times n_e-1$ equations in $5\times n_e+1$ unknowns, i.e., the coefficients $r_j^{(i)}$, $i=1,...,n_e$

and $j = 1,...,4$.

In order to get a solution, the above conditions are completed with two suitable boundary conditions. In particular, the boundary conditions corresponding to the maximum horizontal thrust are straightforward: the maximum thrust is attained when the thrust line is tangent to the intrados in correspondence of the key section of the arch and to the extrados at the imposts, that is:

$$\xi\left(x=0\right)=+\frac{d}{2},\quad \xi\left(x=-1200\right)=-\frac{d}{2}. \tag{62}$$

On the other hand, at the minimum horizontal thrust solution the thrust line is tangent to the extrados in correspondence of the key section of the arch, while it is not known a priori the position of the tangency points at the intrados near the imposts. Thus, the optimization procedure described in Section 5 is employed for determining the minimum thrust solution, and it is found that the tangency points at the intrados near the imposts are attained in correspondence of the cross-sections inclined of $\theta_0 \simeq \pm 63°$ about the vertical axis.

The numerical solutions obtained by the proposed innovative approach are now validated by the comparison with analytical solutions. Given that the solutions of $(55)_1$ and $(55)_2$ have been already determined in closed form, again only equation $(55)_3$ have to be solved. To this aim, since for circular arches the center of curvature of the mid-line is fixed, it is convenient to transform equation $(55)_3$ in polar coordinates; in particular, by applying the relations in Section 3, it results:

$$V\frac{dx}{d\theta}-H\frac{dy}{d\theta}-\gamma\ t\ d\ R_m\left(\xi+\frac{d^2}{12\,R_m}\right)\sin\theta=0 \tag{63}$$

(see also (Ricci et al., 2017)). Then, by setting $q=\gamma\ t\ d\ R_m$, the following analytical solution is obtained:

$$R\left(\theta\right)=\frac{c-q\left(R_m+\dfrac{d^2}{12\,R_m}\right)\cos\theta}{q\ \theta\ \sin\theta+H_o\ \cos\theta} \tag{64}$$

where *c* is an integration constant. Notice that (64) determines the position of the thrust line through its distance from the center of curvature $R(\theta)$, instead of its eccentricity $\xi\left(x\right)$ with respect to the mid-line; but, these quantities are related by (23). Named R_o the radius of the thrust line at $\theta=0$, that is $R\left(\theta=0\right)=R_o$, it is:

$$c=H_o\ R_o+q\left(R_m+\frac{d^2}{12\,R_m}\right); \tag{65}$$

thus, the solution (64) takes the form:

$$R(\theta)=\frac{H_o\ R_o+q\left(R_m+\dfrac{d^2}{12\,R_m}\right)(1-\cos\theta)}{q\ \ \theta\ \sin\theta+H_o\ \ \cos\theta}, \tag{66}$$

and it is expressed in terms of two parameters, the radius of the thrust line at $\theta=0$ and the horizontal thrust H_0. The latter parameters can be determined by imposing suitable boundary conditions. In particular, for obtaining the maximum thrust solution the boundary conditions to be considered for (66) are:

$$R(\theta=0)=R_{in},\qquad R\left(\theta=\frac{\pi}{2}\right)=R_{ex}. \tag{67}$$

The corresponding values of the parameters R_0 and H_0 are:

$$H_0=\frac{q\left(\dfrac{\pi}{2}R_{ex}-R_m-\dfrac{d^2}{12R_m}\right)}{R_0},\qquad R_0=R_{in} \tag{68}$$

On the other hand, the boundary conditions for obtaining the minimum thrust solution are:

$$R(\theta=0)=R_{ex},\qquad R(\theta=\theta_0)=R_{in} \tag{69}$$

where $\theta_0\simeq 63°$ is the angle of the tangency points of the thrust line at the intrados near the imposts before numerically determined. By substituting (69) in (66), it results:

$$H_0=\frac{q\left(R_m+\dfrac{d^2}{12R_m}\right)\left[1-\cos(\theta_0)\right]-R_{in}\ q\ \theta_0\ \sin(\theta_0)}{R_{in}\ \cos(\theta_0)-R_0},\qquad R_0=R_{ex}. \tag{70}$$

Now, the numerical solutions corresponding to the minimum and maximum thrust at the imposts obtained by applying the proposed numerical approach are compared with those analytically determined.

In particular, for what concerns the maximum thrust solution, the value of the thrust at the imposts determined by the numerical procedure is 344.0 kN; this value is practically the same of the value analytically determined by $(67)_1$, that is, H_0=341.9 kN. Moreover, in Fig. a comparison between the analytically determined thrust line (dotted line), obtained from (65) and (67), and the thrust line obtained from the numerical results (solid line) is presented. It can be remarked that the two curves are almost identical.

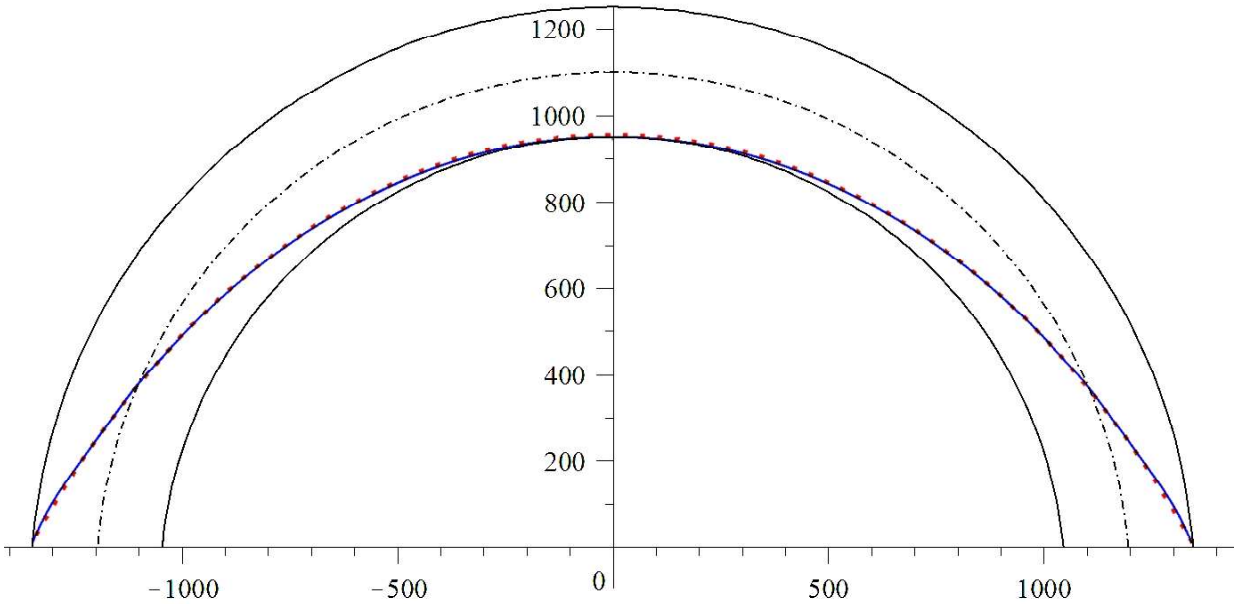

Fig. 5. Maximum thrust solution: analytical (dotted line) and numerical (solid line) results; distances in mm.

For what concerns the minimum thrust solution, the value of the thrust at the imposts determined by the numerical procedure is 155.0 kN; this value is very close to the value analytically determined by $(69)_1$, that is, H_0=152.5 kN. Furthermore, Fig. compares the analytically determined thrust line (dotted line), obtained from (65) and (69), and the thrust line obtained from the numerical results (solid line). Also in this case the two curves are almost identical.

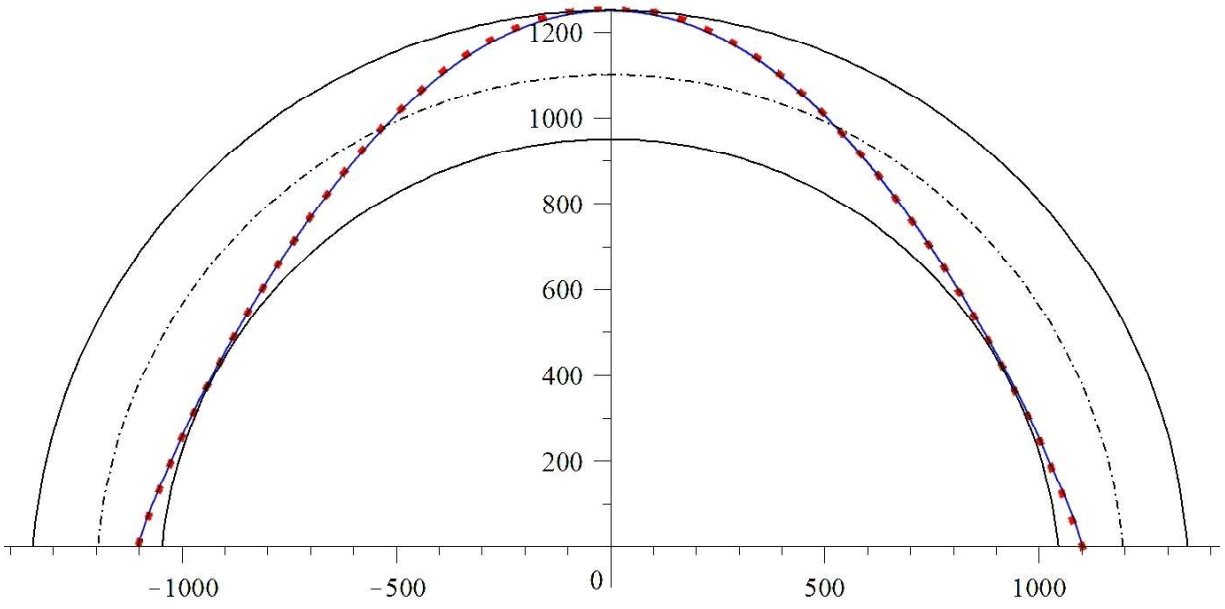

Fig. 6. Minimum thrust solution: analytical (dotted line) and numerical (solid line) results; distances in mm.

The very good match between analytical and numerical solutions proves the effectiveness of the proposed procedure in determining approximated solutions for the differential equation $(55)_3$.

5.2. Parabolic arch

The parabolic arch characterized by the geometric properties reported in Table 2 and subjected to the self-weight is analyzed.

For a parabolic arch the center of curvature is not unique and does not coincide with the center of the global reference system. This complicates the problem of the determination of the thrust line, and no analytical solutions for the this case are available. Then, in order to validate the proposed numerical approach, a comparison between the obtained results and those determined by a FEM code based on the application of the Timoshenko's beam theory for no-tension materials is performed.

Table 2. Geometric data of the parabolic arch.

Mid-line		Extrados		Intrados		d	t	γ
Rise [mm]	Span [mm]	Rise [mm]	Span [mm]	Rise [mm]	Span [mm]	[mm]	[mm]	[daN/mm^3]
1600	3200	1750	3500	1450	2900	300	500	2000

For the considered case-study, the equation of the mid-line curve is:

$$y_m = ax^2 + bx + c \tag{71}$$

with $a = -1/c,\ b = 0,\ c = 1600$ (from now on the distances are expressed in mm). The curvature and the mid-line radius can be determined by (21) and (23), respectively, resulting:

$$k_m = \frac{1}{800\left(1+\frac{1}{640000}x^2\right)^{\frac{3}{2}}}, \qquad R_m = 800\left|1+\frac{1}{640000}x^2\right|^{\frac{3}{2}}. \tag{72}$$

The domain on which the independent variable x is defined is $[-1600,1600]$; this domain is divided in $n_e = 5$ intervals of the same length $\Delta x = 640$.

As the only load is the self-weight, the following positions are made:

$$\gamma(\theta) = \text{cost} = \gamma, \qquad \gamma_h(\theta) = f_e(\theta) = p_e(\theta) = f_i(\theta) = p_i(\theta) = 0. \tag{73}$$

Therefore, the ODE system (47), taking into account the symmetry of the scheme, gives:

$$H = H_0$$

$$V = \gamma\ t\ d\ R_m\ \arctan\left(y'_m\right) \tag{74}$$

$$\frac{1}{\omega}\left(H_0 + V\ y''_m\right)\frac{d\xi}{dx} + \left[-H_0\ \frac{y'_m\ y''_m}{\omega^3} + V\ \frac{y''_m}{\omega^3} + \gamma\ t\ d\ y'_m\right]\xi + H_0\ y'_m - V + \gamma\ y'_m\ \frac{t\ d^3}{12}\ \frac{y''_m}{\omega^3} = 0$$

with H_0 the horizontal thrust, which is constant and unknown, and:

$$y'_m = 2a\ x = \frac{x}{800}$$

$$y''_m = 2a = \frac{1}{800}$$

$$\omega = \sqrt{1+\left(y'_m\right)^2} = \sqrt{1+\frac{x^2}{6.4\cdot 10^5}} \tag{75}$$

$$V = 2.4\cdot 10^7\left(1+\frac{1}{6.4\cdot 10^5}x^2\right)^{3/2}\arctan\left(\frac{x}{800}\right).$$

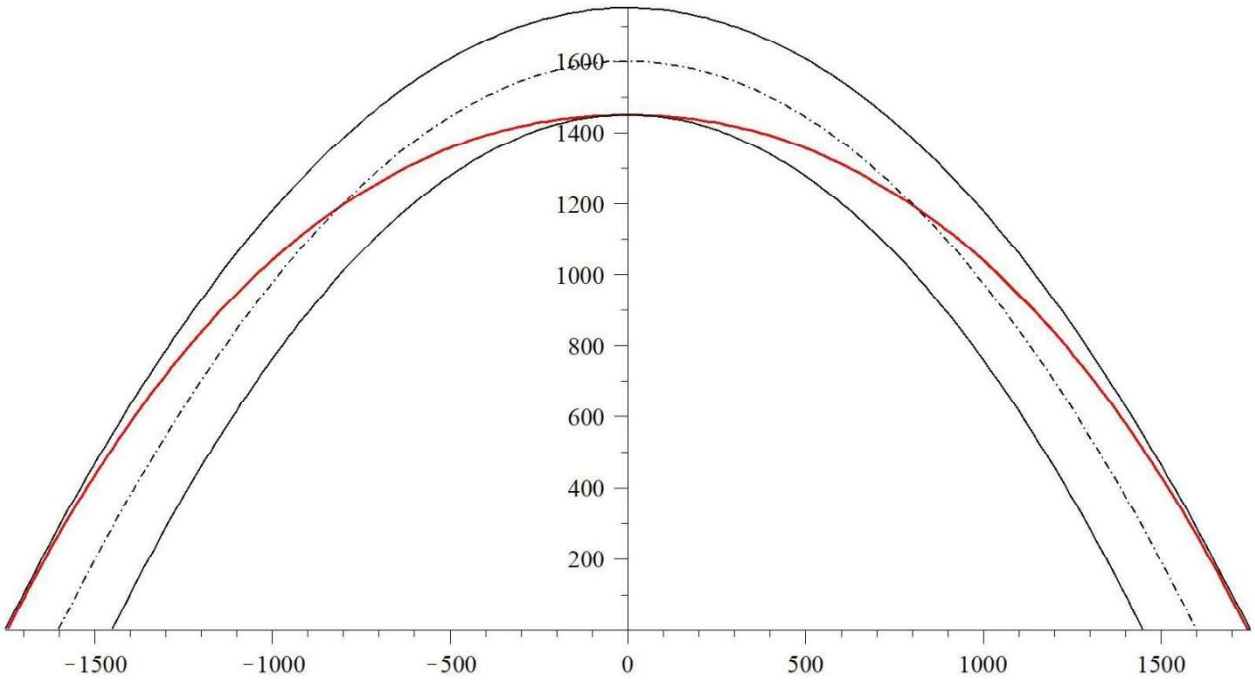

Fig. 7. Thrust line corresponding to the maximum value of the thrust H for a parabolic arch; distances in mm.

For numerically solving $(74)_3$, the unknown function $\xi(x)$ is approximated with a polynomial of fourth degree (see (49)) in each of the 5 intervals. Then, it is required that equation $(74)_3$ is exactly satisfied by the approximating polynomials at the collocation points (51). Moreover, the continuity conditions (52) are imposed. This way, a system of 24 equations in 26 unknowns is obtained. Particular solutions can be determined by imposing two suitable boundary conditions. Among them, the maximum thrust solutions are of interest for applications, corresponding to the following

boundary conditions, expressing the requirements that the thrust line is tangent to the intrados at the crown and intersects the extrados at the imposts:

$$\xi\left(x=0\right)=+\frac{d}{2},\qquad \xi\left(x=-1600\right)=-\frac{d}{2}. \tag{76}$$

This way, a horizontal thrust $H_0 = 404.9$ kN is obtained along with the thrust line shown in Fig. .

For the minimum thrust solution, the following boundary conditions:

$$\xi\left(x=0\right)=-\frac{d}{2},\qquad \xi\left(x=-1600\right)=+\frac{d}{2}, \tag{77}$$

expressing the requirements that the thrust line is tangent to the extrados at the crown and intersects the intrados at the imposts, are imposed. In this case, a horizontal thrust $H_0 = 220.1\cdot10^4$ kN and the thrust line shown in Fig. are obtained.

Now, for validating the obtained numerical solutions, a comparison with the solutions recovered by a FEM implementation of the Timoshenko's beam theory for no-tension materials has been used. Notice that the finite element method considers not only the equilibrium (like the approach here proposed), but also the constitutive equation and the compatibility between displacements and deformations. Thus, in order to make possible a comparison, the following strategy is adopted. Arbitrary constraint conditions are prescribed at the imposts and, consequently, the corresponding thrust line and value of the horizontal thrust at the imposts are determined by the FEM code. Then, the proposed numerical approach is applied by imposing as the boundary conditions exactly the horizontal thrust at the imposts and the eccentricity of the thrust line in two convenient cross-sections evaluated by the FEM analysis. Finally, the two numerical solutions in terms of line of thrust are compared.

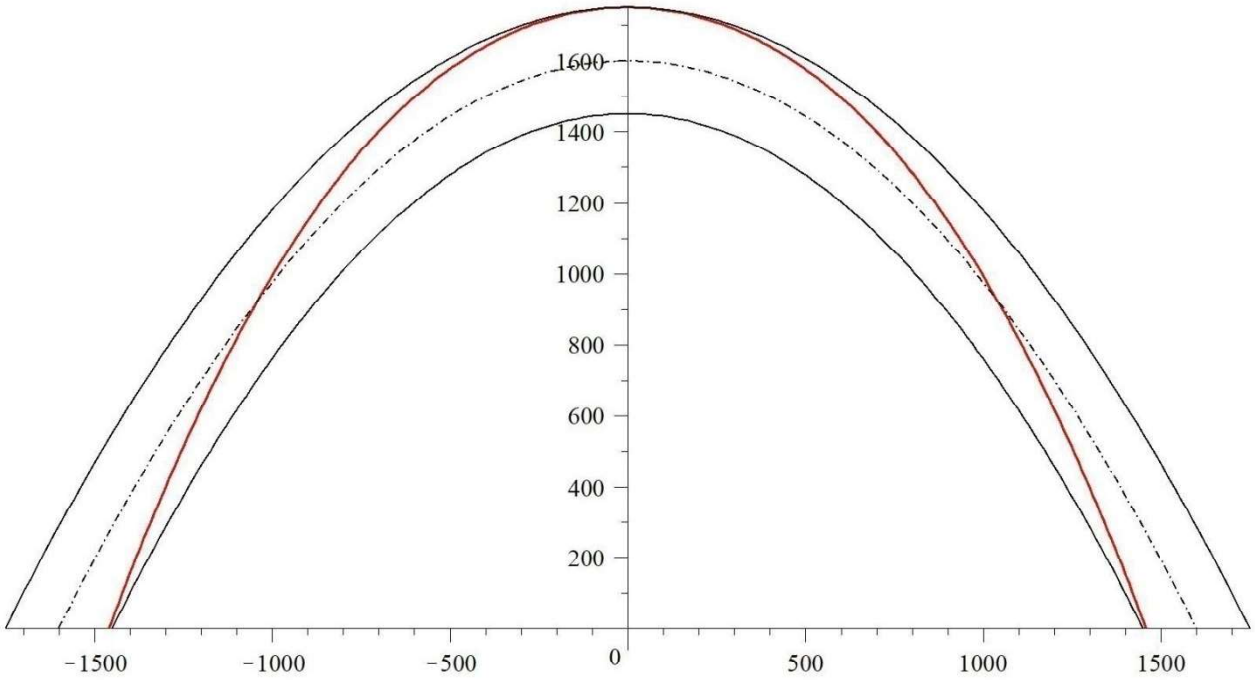

Fig. 8. Thrust line corresponding to the minimum value of the thrust H for a parabolic arch; distances in mm.

In particular, by using the no-tension FEM code a parabolic arch having the features in Table 2 has been solved with the kinematical constraints of clamped imposts. The results given by the FEM code consist not only in the thrust line, but also in the value of the constraints reactions; the horizontal component of these reactions is the thrust at the imposts.

Then, the proposed innovative numerical approach has been applied for determining the thrust line by imposing the following two boundary conditions: 1) the thrust at the imposts is the same of that determined by the Timoshenko's beam no-tension FEM code, that is, 290.1 kN; 2) the eccentricity of the thrust line at the left impost is the same of that determined by the FEM code.

In Fig. the thrust lines determined by the FEM code and by the proposed innovative numerical approach are compared. It is seen that the two curves are practically superimposed: this validate the proposed approach.

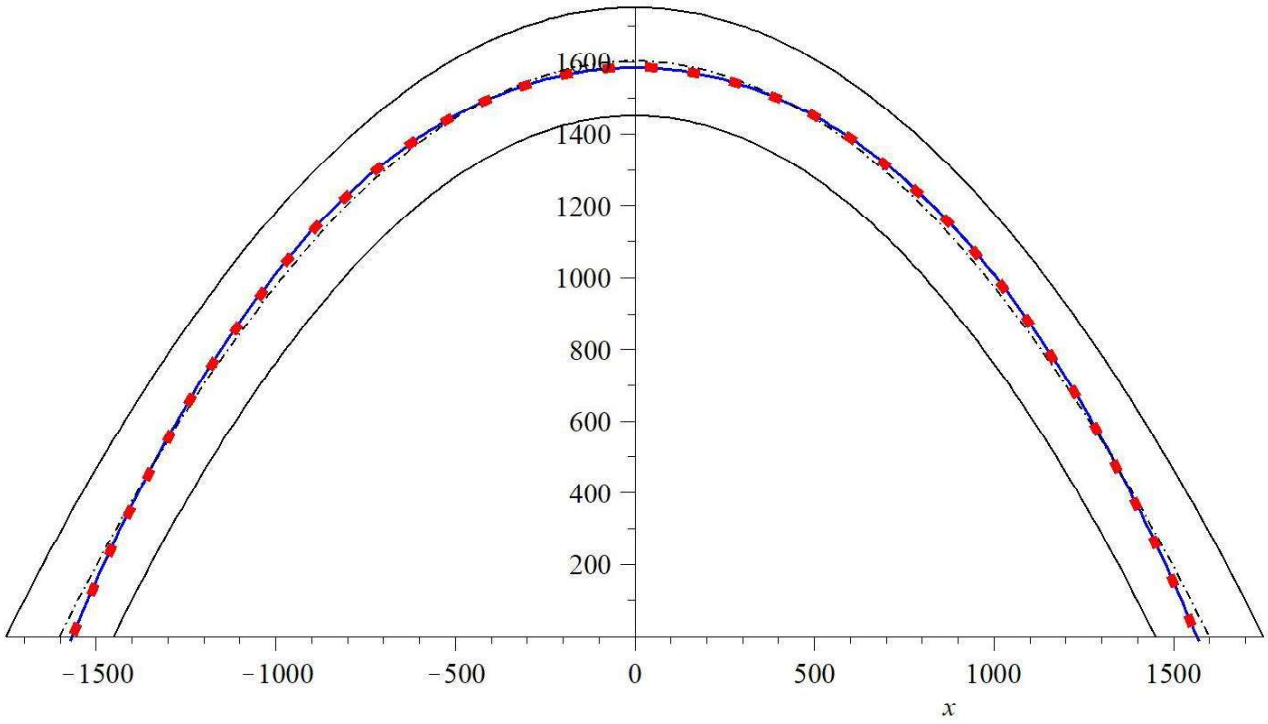

Fig. 9. Comparison between the solutions determined with the FEM (red dotted line) and the PCM (blue solid line); distances in mm.

5.3. Pointed arch subjected to self-weight

A pointed arch subjected to the self-weight, with $\gamma = 2000$ daN/mm^3 and having the geometrical features in Table 3 is considered.

Table 3. Geometric data of the pointed arch.

Mid-line			Extrados			Intrados			C [mm]	*d* [mm]	*t* [mm]
Rise [mm]	Span [mm]	R_m [mm]	Rise [mm]	Span [mm]	R_{ex} [mm]	Rise [mm]	Span [mm]	R_{in} [mm]			
1632	1995	2000	1803	2295	2150	1456	1695	1850	$(\pm 1000, -100)$	300	500

In this case the mid-line equation is piece-wise defined; in particular, each half of the arch is a circular arch whose center does not coincide with the center of the global reference system. Specifically, it results:

$$y_m = y_C + \sqrt{R_m^2 - (x - x_C)^2} \tag{78}$$

with

$$\begin{array}{ll} C\left(+1000,100\right) & if \quad x \le 0 \\ C\left(-1000,100\right) & if \quad x > 0. \end{array} \tag{79}$$

Notice that from now on the distances are expressed in mm. Therefore, the equation of the mid-line is:

$$y_m = \begin{cases} 100 + \sqrt{2000^2 - \left(x-1000\right)^2} & x \le 0 \\ 100 + \sqrt{2000^2 - \left(x+1000\right)^2} & x > 0, \end{cases} \tag{80}$$

and it results:

$$y_m^{'} = \begin{cases} \dfrac{x-1000}{\sqrt{2000^2 - \left(x-1000\right)^2}} & x \le 0 \\ \dfrac{x+1000}{\sqrt{2000^2 - \left(x+1000\right)^2}} & x > 0 \end{cases} \tag{81}$$

and

$$y_m^{''} = \begin{cases} -\dfrac{\left(x-1000\right)^2}{\sqrt{\left[2000^2 + \left(x-1000\right)^2\right]^3}} + \dfrac{1}{\sqrt{2000^2 + \left(x-1000\right)^2}} & x \le 0 \\ -\dfrac{\left(x+1000\right)^2}{\sqrt{\left[2000^2 + \left(x+1000\right)^2\right]^3}} + \dfrac{1}{\sqrt{2000^2 + \left(x+1000\right)^2}} & x > 0. \end{cases} \tag{82}$$

Since also in this case only the action of the self-weight it is considered, positions (73) hold and the ODE system (47) reduces again to (74).

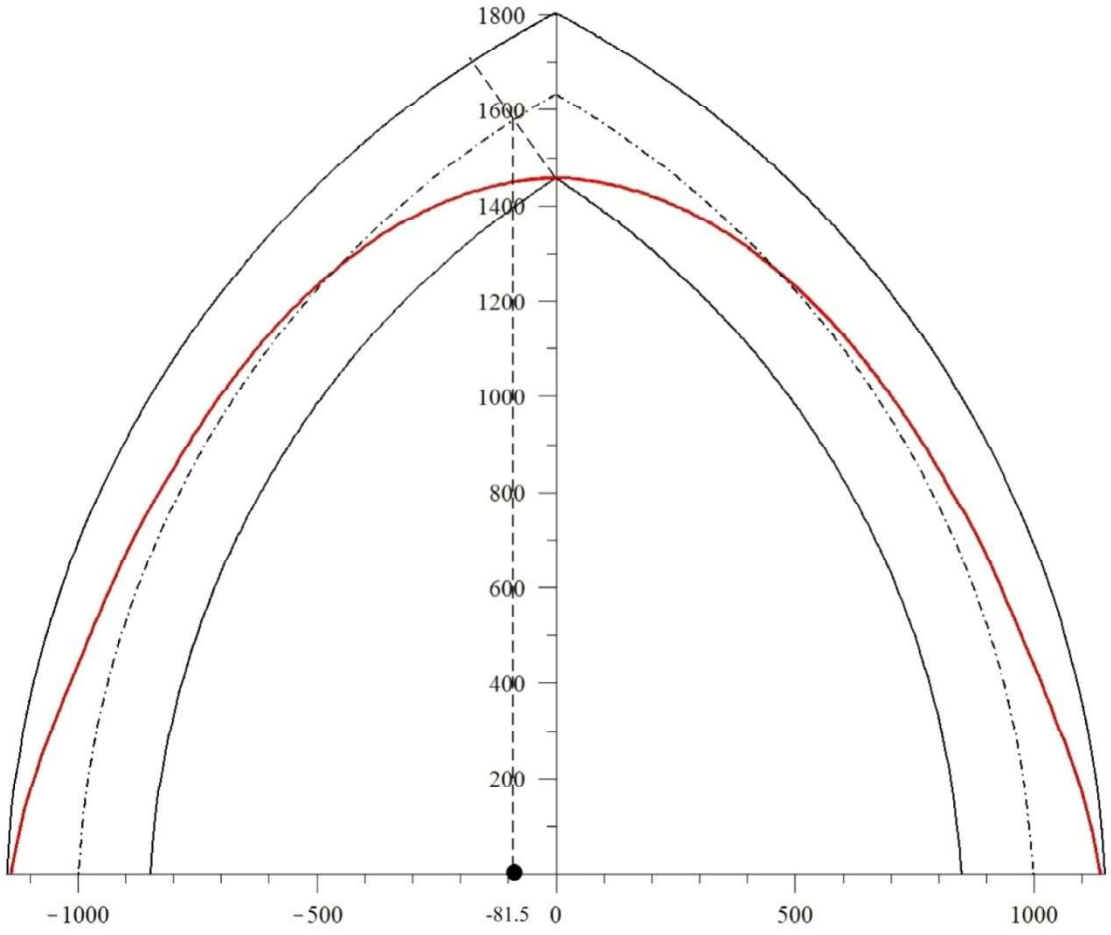

Fig. 10. Thrust line corresponding to the maximum value of the thrust H for a pointed arch; distances in mm.

From the geometry it is possible to infer that the domain of the independent variable x is [-997.5, 997.5]; for the numerical calculations this domain is divided in $n_e = 8$ intervals. For each interval the function $\xi(x)$ has been approximated with the fourth degree polynomial (49). Then, it is required that equation $(74)_3$ is exactly satisfied by the approximating polynomials at the collocation points (51). Moreover, the continuity conditions (52) are imposed. In this way, accounting for the symmetry of the scheme, a system of 39 equations in 41 unknowns it is obtained. Particular solutions can be determined by imposing two suitable boundary conditions.

Indeed, in order to determine the maximum value of the horizontal thrust the conditions that the thrust line is tangent to the intrados at the crown and to the extrados at the imposts are imposed, that is:

$$\xi\left(x=-81.5\right)=+\frac{d}{2}, \qquad \xi\left(x=-997.5\right)=-\frac{d}{2}. \tag{83}$$

For what concerns $(83)_1$, it is worth recalling that the independent variable x is referred to the mid-line: thus, condition $(83)_1$ refers to the point of the mid line from which passes the cross-section corresponding to the point of the intrados at the crown of the arch (see Fig.). This way, it is

determined a maximum value of the thrust $H_0 = 210.2$ kN. In Fig. the thrust line corresponding to this solution it is plotted.

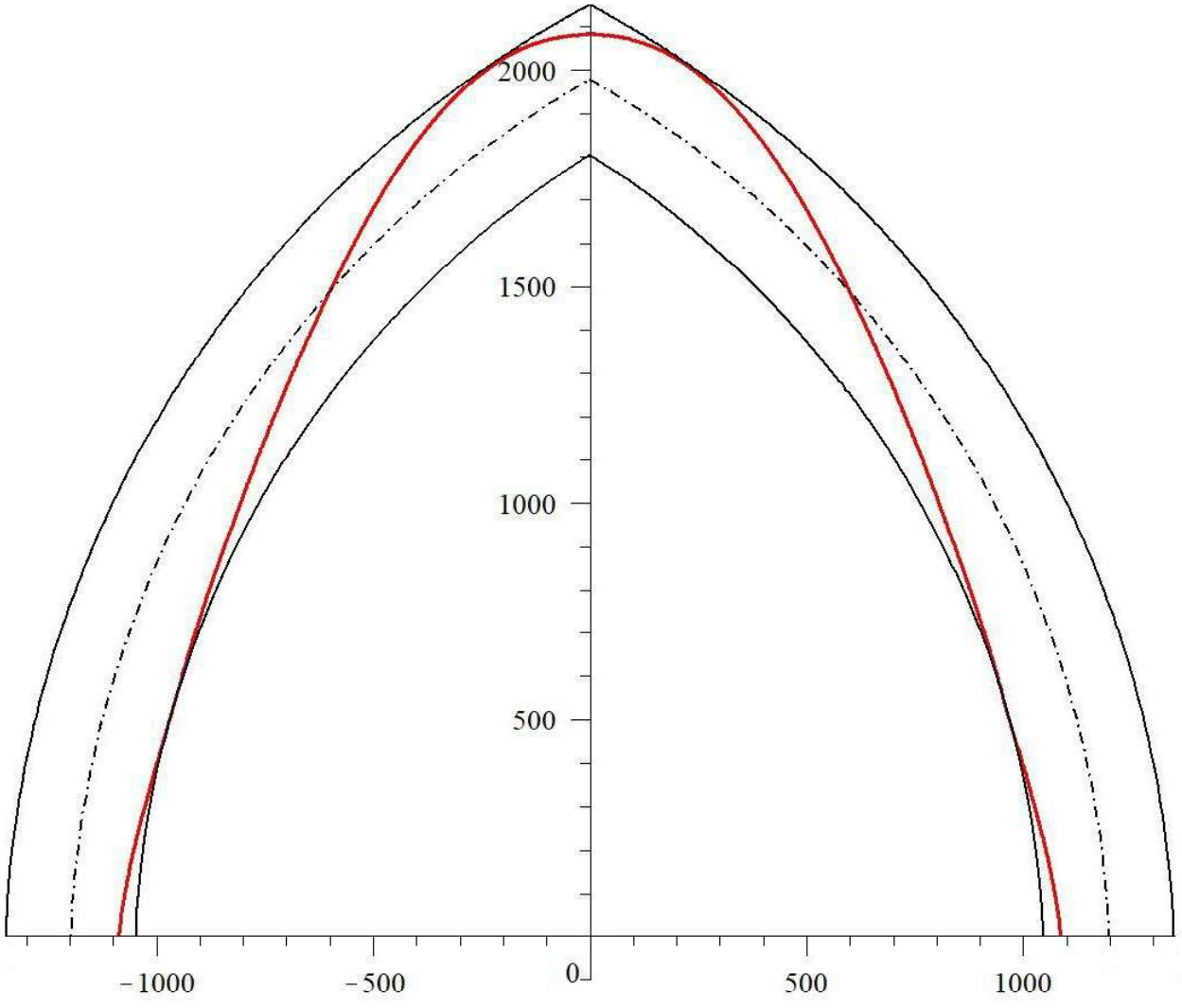

Fig. 11. Thrust line corresponding to the minimum value of the thrust H for a pointed arch; distances in mm.

For determining the minimum thrust solution, the thrust line must be tangent to the extrados in two points near the crown and to the intrados near the imposts. Nevertheless, the position of the tangency points near the imposts and the crown are not known in advance. Thus, the optimization procedure described in Section 4 has been employed for the determination of the minimum thrust solution. In particular, the minimum value of the horizontal thrust has been found to be $H_0 = 112.9$ kN. In Fig. the curve corresponding to the minimum value of H_0 has been plotted.

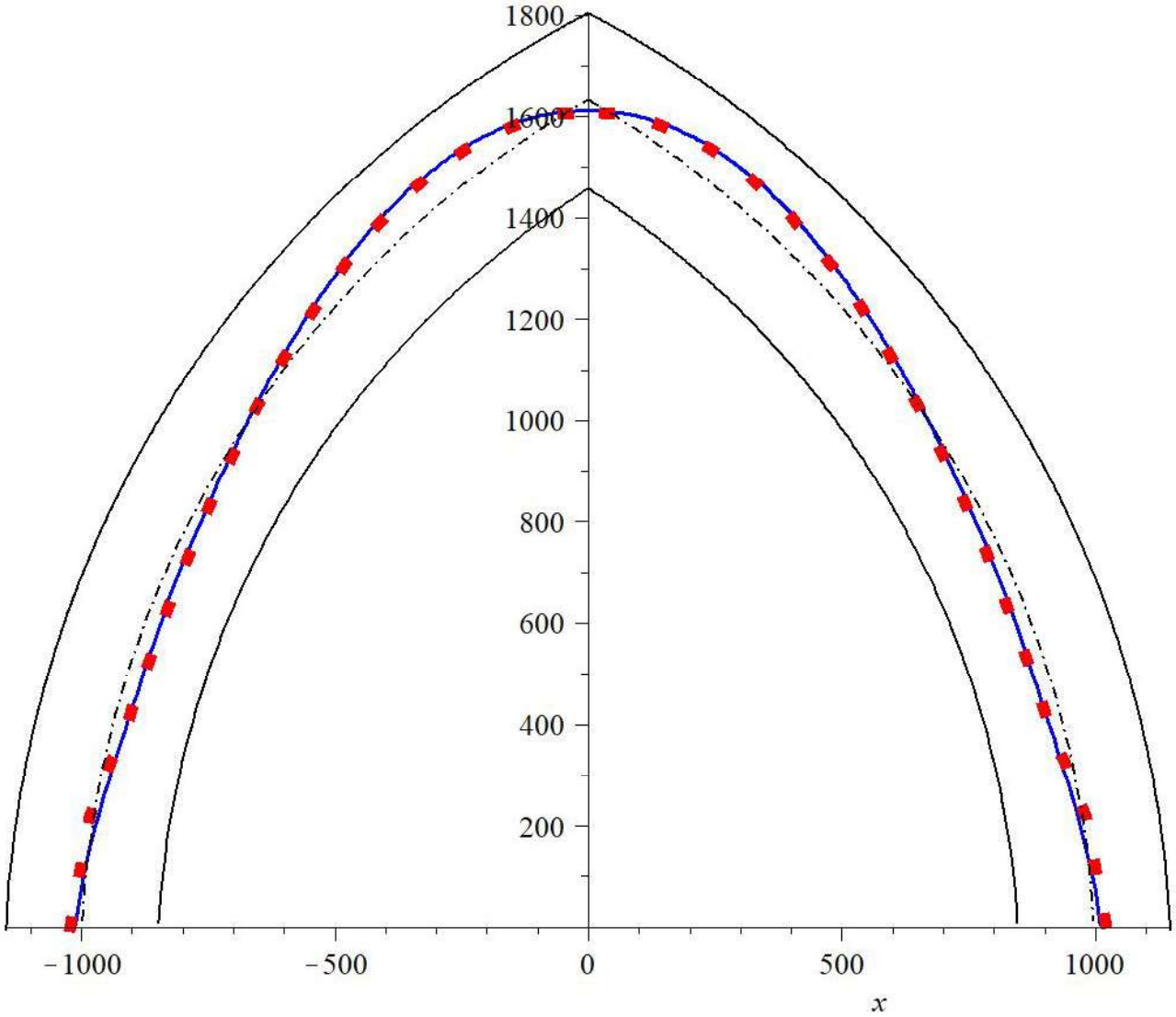

Fig. 12. Comparison between the FEM solution and the PCM solution; distances in mm.

In order to validate the obtained numerical solutions a comparison with the solution obtained by the Timoshenko's beam no-tension FEM code has been determined. In particular, by following the same approach discussed in previous section for the parabolic arch, a pointed arch having the geometrical data in Table 3 and clamped at the imposts has been analyzed by the FEM code. Then, the proposed innovative numerical approach has been applied by imposing the following boundary conditions: 1) the thrust at the imposts is the same of that determined by the FEM code, that is, 140.5 kN; 2) eccentricity of the thrust line at the left impost is the same of that determined by the FEM code.

In Fig. the thrust lines determined by the Timoshenko's beam no-tension FEM code and by the proposed innovative numerical approach are compared. Also in this case, it is clear that the two curves practically coincide: this further validate the approach here proposed.

6. Conclusions

The Milankovitch's theory of equilibrium of masonry arches is revisited and generalized within the framework of Limit Analysis applied to masonry structures. The generalization involves the geometrical description of the problem, more consistent with the data obtainable from a field survey, and the loading condition: indeed, also horizontal inertial forces representing seismic loads have been considered. Moreover, a numerical procedure based on a suitable implementation of the Point Collocation Method for determining solutions of the equilibrium problem has been developed, as solutions are often analytically infeasible. A key aspect of the proposed numerical procedure is a constrained optimization routine that may be used for determining, among the infinity of equilibrium solutions, those of special interest for applications. For example, maximum and minimum thrust solutions can be determined, but also the geometric safety factor, or the collapse load multiplier for variable loads, even in the case of horizontal seismic loads.

This innovative formulation aims at making available the most advanced and accurate theory of equilibrium for masonry arches for determining optimal Limit Analysis solutions from the “safe” side (Lower-Bound theorem of Limit Analysis).

The proposed approach is applied for studying masonry arches under the self-weight, and the attention is focused on maximum and minimum thrust solutions. The obtained solutions are validated both by the comparison with analytical solutions (for the circular arch) and by the comparison with numerical solutions obtained by using a Timoshenko's beam no-tension FEM code. The results of the comparisons show the effectiveness of the proposed approach: the thrust lines obtained by the latter are substantially superimposed to the reference thrust lines.

This encourages further studies on the application of the proposed approach to masonry arches under more general load conditions, including also horizontal seismic loads, and on reinforced masonry arches.

7. References

Addessi, D., Sacco, E., 2014. A kinematic enriched plane state formulation for the analysis of masonry panels. Eur. J. Mech. A/Solids 44, 188–200.

Addessi, D., Sacco, E., Paolone, A., 2010. Cosserat model for periodic masonry deduced by nonlinear homogenization. Eur. J. Mech. A/Solids. https://doi.org/10.1016/j.euromechsol.2010.03.001

Ageno, A., Bernabo, A., Foce, F., Sinopoli, A., 2004. Theory and History of the Thrust Line for Masonry Arches. A Brief Account. Proc. 4th Int. Conf. Arch Bridg. 1–10.

Alecci, V., Focacci, F., Rovero, L., Stipo, G., de Stefano, M., 2016a. Extrados strengthening of brick masonry arches with PBO-FRCM composites: Experimental and analytical investigations. Compos. Struct. https://doi.org/10.1016/j.compstruct.2016.04.030

Alecci, V., Focacci, F., Rovero, L., Stipo, G., De Stefano, M., 2017. Intrados strengthening of brick masonry arches with different FRCM composites: Experimental and analytical investigations. Compos. Struct. https://doi.org/10.1016/j.compstruct.2017.06.023

Alecci, V., Misseri, G., Rovero, L., Stipo, G., De Stefano, M., Feo, L., Luciano, R., 2016b. Experimental investigation on masonry arches strengthened with PBO-FRCM composite. Compos. Part B Eng. https://doi.org/10.1016/j.compositesb.2016.05.063

Angelillo, M., Fortunato, A., Montanino, A., Lippiello, M., 2014. Singular stress fields in masonry structures: Derand was right. Meccanica. https://doi.org/10.1007/s11012-014-9880-6

Baraldi, D., Cecchi, A., 2016. Discrete approaches for the nonlinear analysis of in plane loaded masonry walls: Molecular dynamic and static algorithm solutions. Eur. J. Mech. A/Solids. https://doi.org/10.1016/j.euromechsol.2015.12.008

Baraldi, D., Cecchi, A., Tralli, A., 2015. Continuous and discrete models for masonry like material: A critical comparative study. Eur. J. Mech. A/Solids. https://doi.org/10.1016/j.euromechsol.2014.10.007

Benvenuto, E., 1981. La scienza delle costruzioni e il suo sviluppo storico. Sansoni, Firenze.

Bertolesi, E., Milani, G., Carozzi, F.G., Poggi, C., 2018a. Ancient masonry arches and vaults strengthened with TRM, SRG and FRP composites: Experimental evaluation. Compos. Struct. 187, 466–480. https://doi.org/10.1016/j.compstruct.2017.12.075

Bertolesi, E., Milani, G., Carozzi, F.G., Poggi, C., 2018b. Ancient masonry arches and vaults strengthened with TRM, SRG and FRP composites: Numerical analyses. Compos. Struct. 187, 385–402. https://doi.org/10.1016/j.compstruct.2017.12.021

Block, P., Dejong, M., Ochsendorf, J., 2006. As hangs the flexible line: Equilibrium of masonry arches. Nexus Netw. J. 8, 13–24. https://doi.org/10.1007/s00004-006-0015-9

Block, P., Ochsendorf, J.A., 2008. Lower-bound Analysis of Masonry Vaults, in: Structural Analysis of Historic Construction: Preserving Safety and Significance. https://doi.org/10.1201/9781439828229.ch67

Coulomb, C., 1776. Essai sur une application des règles de maximis & minimis à quelques problèmes de statique, relatifs à l'architecture. De l'Imprimerie Royale, Paris.

Couplet, P., 1732. Seconde partie de l'éxamen de la poussée des voûtes, in: Mémoires de l'Académie Royale Des Sciences, Année 1730. pp. 117–141.

Couplet, P., 1731. De la poussée des voûtes, in: Mémoires de l'Académie Royale Des Sciences, Année 1729. pp. 79–117.

D'Altri, A.M., Castellazzi, G., de Miranda, S., 2018. Collapse investigation of the Arquata del Tronto medieval fortress after the 2016 Central Italy seismic sequence. J. Build. Eng. https://doi.org/10.1016/j.jobe.2018.03.021

de La Hire, P., 1720. Sur la construction des voûtes dans les édifices, in: Mémoires de l'Académie Royale Des Sciences, Année 1702. pp. 100–103.

de La Hire, P., 1695. Traité de mécanique, où l'on explique tout ce qui est nécessaire dans la pratique des Arts, et les proprietés des corps pesants lesquelles ont eu plus grand usage dans la Physique. Imprimerie Royale, Paris.

Drougkas, A., Roca, P., Molins, C., 2016. Nonlinear micro-mechanical analysis of masonry periodic unit cells. Int. J. Solids Struct. https://doi.org/10.1016/j.ijsolstr.2015.11.004

Fabbrocino, F., Farina, I., Berardi, V.P., Ferreira, A.J.M., Fraternali, F., 2015. On the thrust surface of unreinforced and FRP-/FRCM-reinforced masonry domes. Compos. Part B Eng. https://doi.org/10.1016/j.compositesb.2015.08.061

Foce, F., 2007. Milankovitch's Theorie der Druckkurven: Good mechanics for masonry architecture. Nexus Netw. J. 9, 185–210. https://doi.org/10.1007/s00004-007-0039-9

Fortunato, A., Babilio, E., Lippiello, M., Gesualdo, A., Angelillo, M., 2016. Limit Analysis for Unilateral Masonry-like Structures. Open Constr. Build. Technol. J. 10, 346–362.

https://doi.org/10.2174/1874836801610010346

Fortunato, A., Fabbrocino, F., Angelillo, M., Fraternali, F., 2017. Limit analysis of masonry structures with free discontinuities. Meccanica 1–10. https://doi.org/10.1007/s11012-017-0663-8

Gilbert, M., 2007. Limit analysis applied to masonry arch bridges: state-of-the-art and recent developments. Proc. 5th Int. Conf. Arch Bridg.

Gregory, D., 1698. Catenaria. Philos. Trans. 19, 637–652.

Heyman, J., 1966. The stone skeleton. Int. J. Solids Struct. https://doi.org/10.1016/0020-7683(66)90018-7

Hooke, R., 1676. A description of helioscopes, and some other instruments. London.

Huerta, S., 2006. Galileo was wrong: The geometrical design of masonry arches. Nexus Netw. J. 8, 25–52. https://doi.org/10.1007/s00004-006-0016-8

Huerta, S., 2004. Arcos, bóvedas y cúpulas : geometría y equilibrio en el cálculo tradicional de estructuras de fábrica. Instituto Juan de Herrera.

Lemos, J. V., 2007. Discrete element modeling of masonry structures. Int. J. Archit. Herit. https://doi.org/10.1080/15583050601176868

Livesley, R.K., 1978. Limit analysis of structures formed from rigid blocks. Int. J. Numer. Methods Eng. https://doi.org/10.1002/nme.1620121207

Lubliner, J., 1990. Plasticity Theory. Macmillan Publishing Company, New York.

Lucchesi, M., Pintucchi, B., Zani, N., 2018. Masonry-like material with bounded shear stress. Eur. J. Mech. / A Solids 72, 329–340. https://doi.org/10.1016/j.euromechsol.2018.05.001

Luciano, R., Sacco, E., 1998. A damage model for masonry structures. Eur. J. Mech. - A/Solids. https://doi.org/10.1016/S0997-7538(98)80087-9

Mascheroni, L., 1785. Nuove ricerche sull'equilibrio delle volte. Locatelli, Bergamo.

Méry, É., 1840. Sur l'équilibre des voûtes en berceau,. Ann. des Ponts Chaussées 19, 50–70.

Milani, G., Lourenço, P.B., 2012. 3D non-linear behavior of masonry arch bridges. Comput. Struct.

https://doi.org/10.1016/j.compstruc.2012.07.008

Milanković, M., 1907. Theorie der Druckkurven. Zeitschrift für Math. und Phys. 55, 1–27.

Milanković, M., 1904. Beitrag zur Theorie der Druckkurven. K.K. technische Hochschule, Wien.

Navier, C.-L., 1826. Résumé des leçons données à l'École des Ponts et Chaussées sur l'application de la mécanique à l'établissement des constructions et des machines. F. Didot père et fils, Paris.

Nikolić, D., 2016. A note on Milankovitch's theory of thrust line applied to gothic masonry arches, in: 4th International Conference Contemporary Achievements in Civil Engineering 22. April 2016. Subotica, SERBIA. https://doi.org/DOI:10.14415/konferencijaGFS 2016.018

Nobile, L., Bartolomeo, V., 2014. Methods for the Assessment of Historical Masonry Arches. Proc. 5th Eur. Conf. Civ. Eng. (ECCIE '14) 160–167.

O'Dwyer, D., 1999. Funicular analysis of masonry vaults. Comput. Struct. https://doi.org/10.1016/S0045-7949(98)00279-X

Oliveira, D. V., Lourenço, P.B., Lemos, C., 2010. Geometric issues and ultimate load capacity of masonry arch bridges from the northwest Iberian Peninsula. Eng. Struct. https://doi.org/10.1016/j.engstruct.2010.09.006

Pintucchi, B., Zani, N., 2016. A simple model for performing nonlinear static and dynamic analyses of unreinforced and FRP-strengthened masonry arches. Eur. J. Mech. A/Solids. https://doi.org/10.1016/j.euromechsol.2016.03.013

Pintucchi, B., Zani, N., 2009. Effects of material and geometric non-linearities on the collapse load of masonry arches. Eur. J. Mech. A/Solids. https://doi.org/10.1016/j.euromechsol.2008.02.007

Ricci, E., Fraddosio, A., Piccioni, M.D., Sacco, E., 2017. Numerical methods for the lower bound limit analysis of masonry arches. AIMETA 2017 - Proc. 23rd Conf. Ital. Assoc. Theor. Appl. Mech. 2.

Ricci, E., Sacco, E., Piccioni, M.D., 2016. A method for the analysis of masonry arches, in: Structural Analysis of Historical Constructions: Anamnesis, Diagnosis, Therapy, Controls - Proceedings of the 10th International Conference on Structural Analysis of Historical Constructions, SAHC 2016. Leuven; Belgium, pp. 1239–1245.

Roca, P., Cervera, M., Gariup, G., Pela', L., 2010. Structural analysis of masonry historical constructions. Classical and advanced approaches. Arch. Comput. Methods Eng. https://doi.org/10.1007/s11831-010-9046-1

Sacco, E., 2015. Some Aspects on the Statics of Masonry Arches, in: Masonry Structures: Between Mechanics and Architecture. Springer International Publishing, Cham, pp. 265–290. https://doi.org/10.1007/978-3-319-13003-3_10

Sarhosis, V., Oliveira, D. V., Lemos, J. V., Lourenco, P.B., 2014. The effect of skew angle on the mechanical behaviour of masonry arches. Mech. Res. Commun. https://doi.org/10.1016/j.mechrescom.2014.07.008

Tralli, A., Alessandri, C., Milani, G., 2014. Computational methods for masonry vaults: A review of recent results. Open Civ. Eng. J. https://doi.org/10.2174/1874149501408010272

Varma, M., Jangid, R.S., Ghosh, S., 2010. Thrust Line Using Linear Elastic Finite Element Analysis for Masonry Structures. Adv. Mater. Res. https://doi.org/10.4028/www.scientific.net/AMR.133-134.503